

Lecture 7

Lecturer: Asst. Prof. M. Mert Ankarali

Mapping Between s & z Planes

When the (uniform) impulse sampling is involved in the process, then we know that s and z variables are related with

$$z = e^{Ts}$$

which is a mapping from complex plane to complex plane, i.e. $M : \mathbb{C} \mapsto \mathbb{C}$, where $M(s) = e^{Ts}$. We will analyze different cases of this mapping and their relevance and importance.

Moreover, if s_p is a pole of $G_p(s)$, then it is straightforward to show that $z_p = e^{Ts_p}$ is a pole of $G(z) = \mathcal{Z}\{G_p(s)\}$ (as well as $G(z) = (1 - z^{-1})\mathcal{Z}\{G(s)/s\}$).

Since poles of an LTI system (CT or DT) are the major features that defines the stability and some other performance metrics, analyzing this mapping is very critical for analyzing discrete time control systems.

Mapping of real line (left half and right half): When s is purely real (i.e. when the roots of the CT plant are real) we have

$$s = \sigma, \sigma \in \mathbb{R}$$

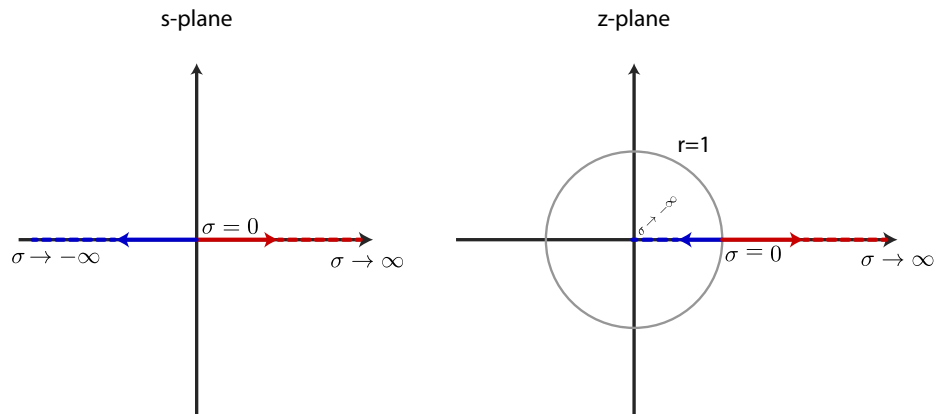
$$z = e^{Ts} = e^{T\sigma}, z \in \mathbb{R}^+$$

It is also easy to see the difference between left half and right half of the real line

$$\text{If } \sigma \leq 0 \rightarrow z = e^{\sigma T} \in [0, 1]$$

$$\text{If } \sigma \geq 0 \rightarrow z = e^{\sigma T} \in [1, \infty)$$

Mapping of both left and right real lines to z-plane is illustrated in the Figure below. It can be seen that when $\sigma > 0$, $z > 1$, and similarly when $\sigma < 0$, $z < 1$. Technically on both planes red curves belong to “unstable” behaviors, whereas blue curves belong to “stable” behaviors.



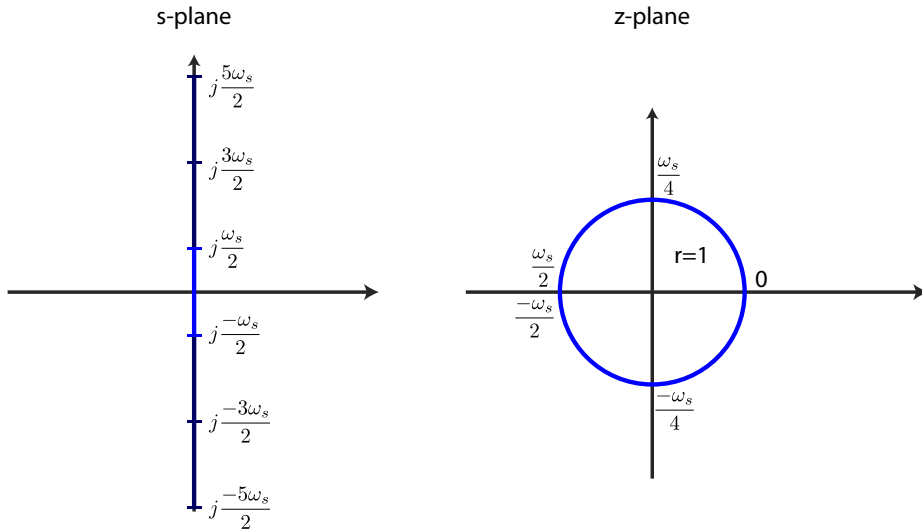
Mapping of imaginary axis: When s is purely imaginary (i.e. when the roots of the CT plant are critically stable) we have

$$\begin{aligned}s &= j\omega \quad , \quad \omega \in \mathbb{R} \\ z &= e^{Ts} = e^{T\omega j} \\ |z| &= 1 \\ \angle z &= T\omega = T\omega + 2\pi k \quad , \quad k \in \mathbb{Z}\end{aligned}$$

This means that mapping of the imaginary axis is not 1-1, since multiple points on s plane can correspond to a single point on the z plane

$$e^{T\omega j} = e^{(T\omega + 2\pi k)j} \rightarrow M(\omega j) = M((\omega + 2\pi k/T)j) = M((\omega + \omega_s k)j) , \quad k \in \mathbb{Z}$$

where $\omega_s = 2\pi/T$ is the sampling frequency. It can be seen that imaginary axis on the s plane is mapped to the unit circle on the z plane. However as $\omega \rightarrow \infty$ or $\omega \rightarrow -\infty$, the mapping circles the unit circle multiple (indeed infinite) times. This mapping is illustrated in the Figure below. The light blue section on the s plane (which covers the points in the imaginary axis between $[-\omega_s/2, \omega_s/2]$) is called the primary section/strip and fully mapped to the unit circle. Dark blue sections are called complementary sections/strips and they are also individually fully mapped onto the unit circle.



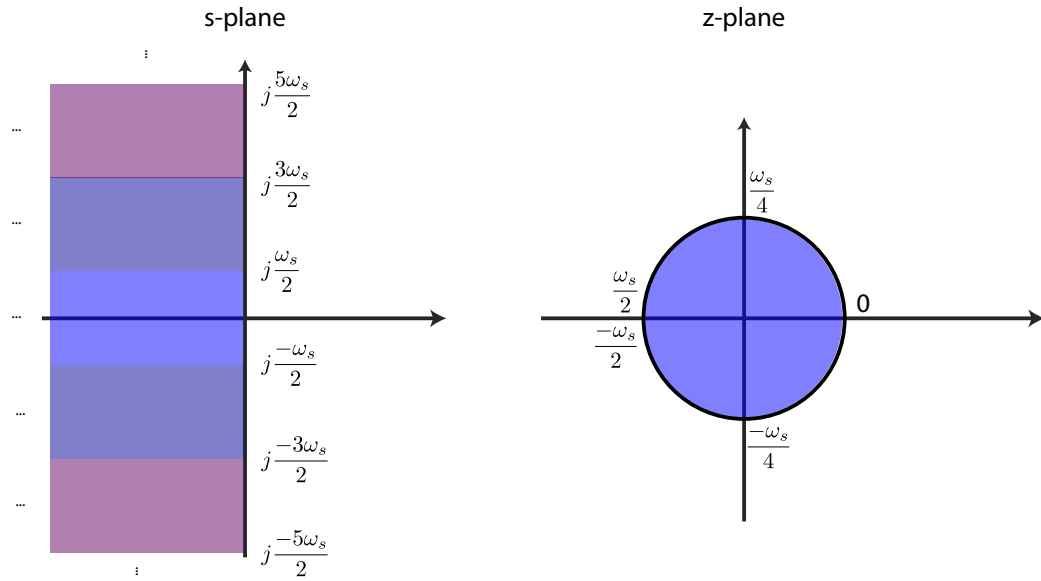
Mapping of open left-half plane: Now let's generalize a little, and consider the mapping of the whole open left-half plane.

$$\begin{aligned}s &= \sigma + j\omega \quad , \quad \sigma < 0 \\ z &= e^{Ts} = e^{T\sigma} e^{T\omega j} = e^{T\sigma} e^{(T\omega + 2\pi k)j} \\ |z| &= e^{T\sigma} < 1 \\ \angle z &= T\omega + 2\pi k \quad , \quad k \in \mathbb{Z}\end{aligned}$$

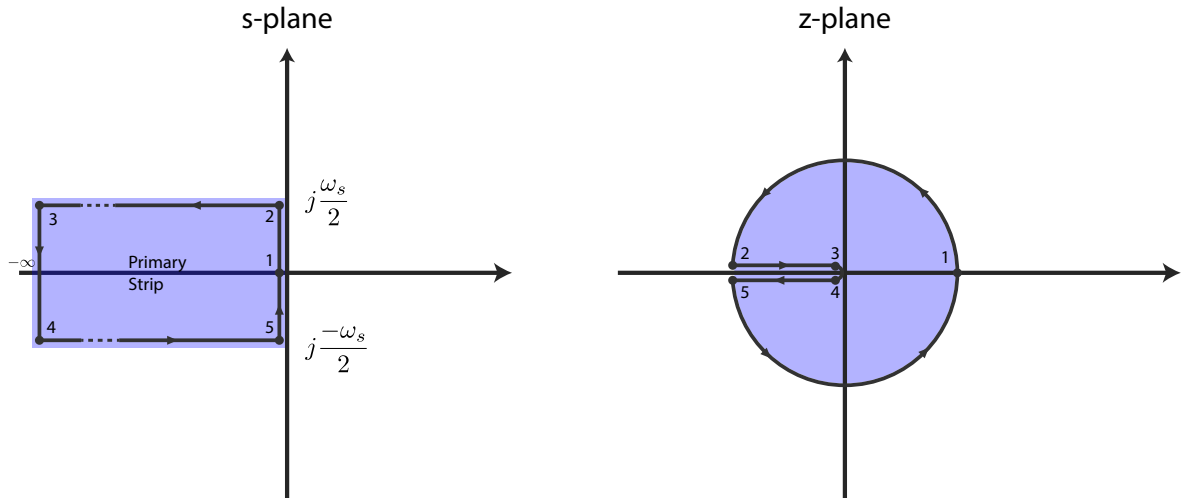
Obviously, this mapping is also not 1-1, and “periodic” in ω , i.e.

$$M(\sigma + \omega j) = M(\sigma + (\omega + 2\pi T)j) = M(\sigma + (\omega + \omega_s)j)$$

Mapping of OLH on s -plane to z -plane is illustrated in Figure below.



In the primary strip, if we trace the path that is defined by the sequence of points 1-2-3-4-5-1 in the s plane as shown in the Figure below, than this path is mapped in to the z-plane as shown in the Figure. The mapping forms a different path again associated with mapped point sequence 1-2-3-4-5-1.

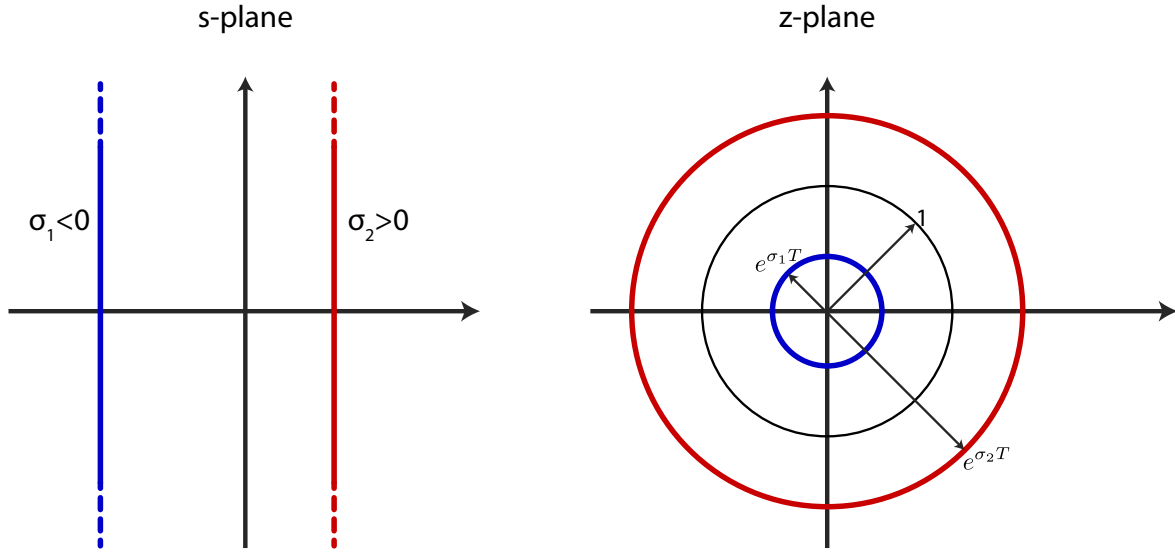


Mapping of constant attenuation line: In the s-plane, it corresponds to the line for which σ is constant. Constant σ in s-plane corresponds to a constant radius in the z-plane. Thus line is mapped to a circle with a radius of $e^{\sigma T}$.

$$z = e^{\sigma T} e^{\omega T j} = e^{\sigma T} \angle \omega T$$

$$R = e^{\sigma T} = \text{Constant}$$

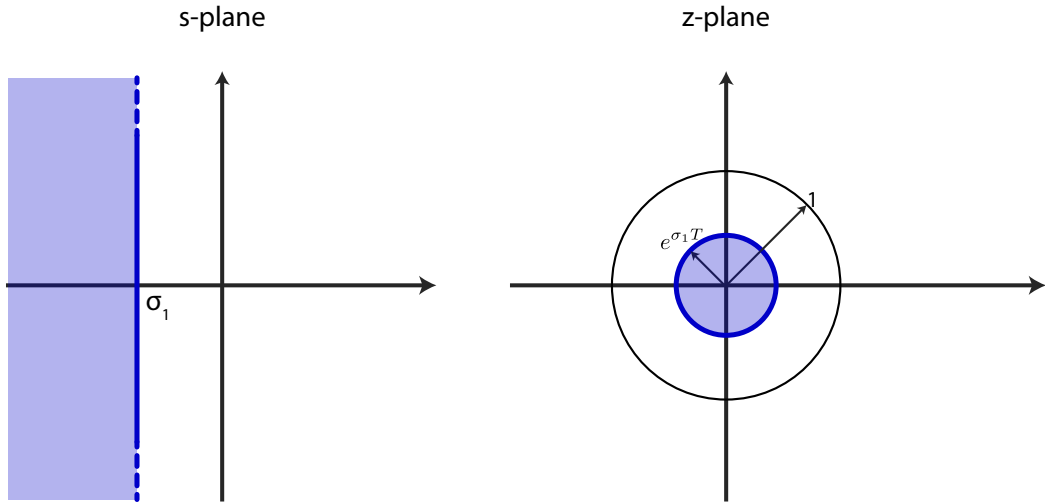
Figure below illustrates mapping of one constant attenuation line in open left half plane and one open right half plane.



Max convergence/settling time region: For a stable CT LTI system convergence/settling time is defined by the real part of the pole. Thus on the s-plane we have the following condition

$$\operatorname{Re}(s) < \sigma_1 < 0$$

In the z-plane it is mapped to region enclosed by the circle with radius $r = e^{\sigma_1 T}$. This mapping is illustrated below.

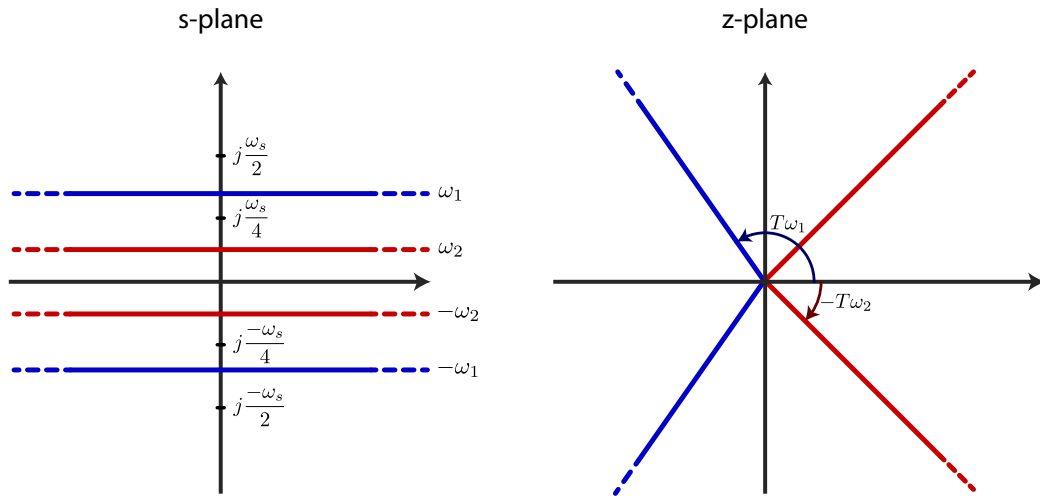


Constant frequency loci: A constant frequency locus $\omega = \omega_1$ in s-plane is mapped to a constant angle line in z-plane, for which the angle is equal to $\omega_1 T$.

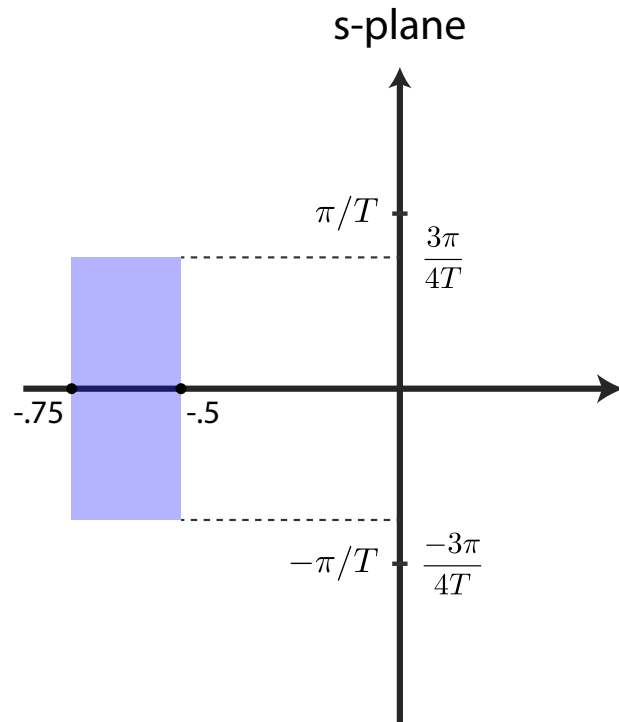
$$z = e^{\sigma T} e^{\omega T j} = e^{\sigma T} \angle \omega T$$

$$\angle \omega T = \text{Constant}$$

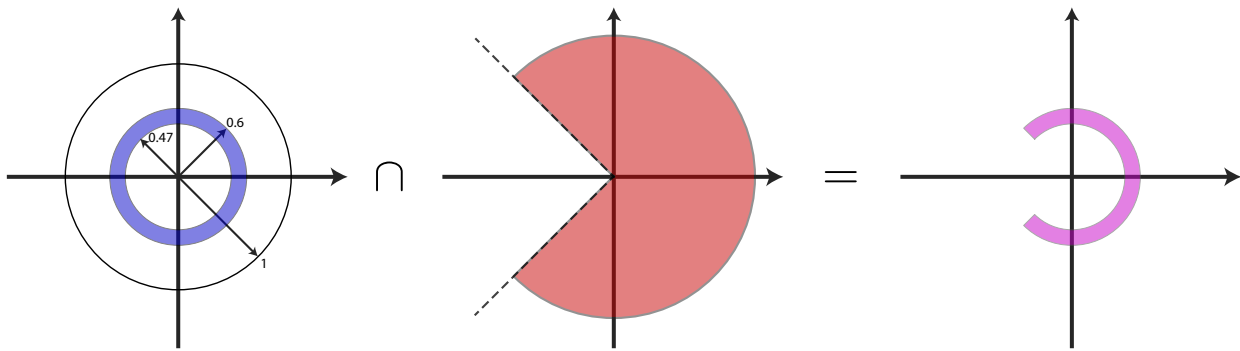
Different constant frequency lines (all inside the primary strip) and their mappings are illustrated in Figure below.



Example: Find the mapping of the area defined inside s-plane illustrated in Figure below with $T = 1$.



Solution: The solution is illustrated in the Figure below



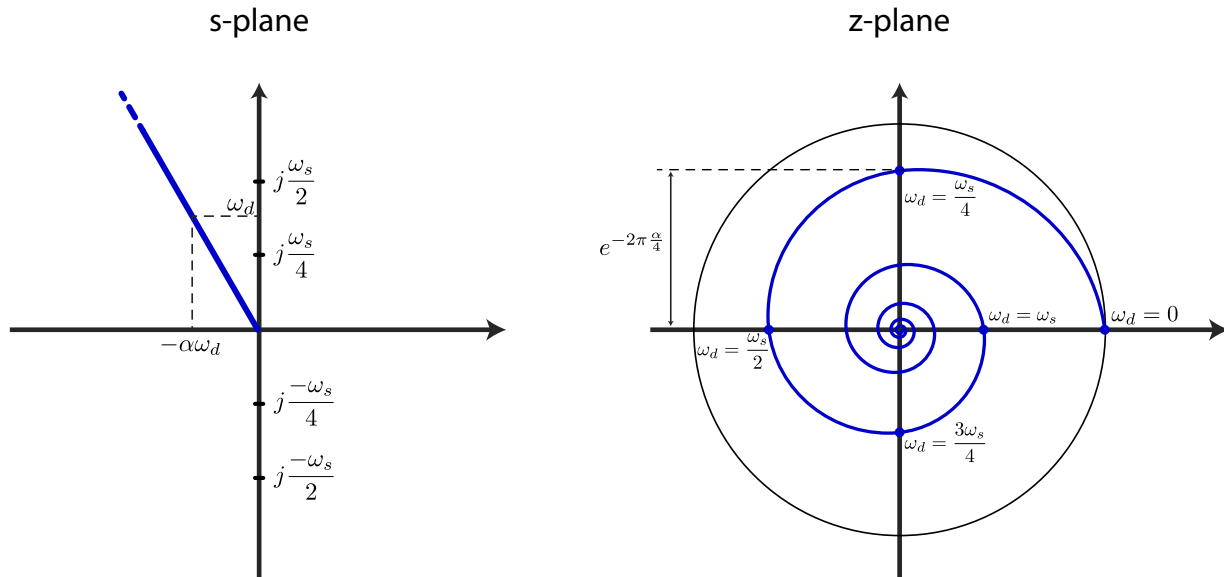
Constant damping loci: A constant damping loci is a line in s-plane passing through the origin and the angle between the line and the Real (or Imaginary) axis defines the damping ratio. In s-plane we have the following relations

$$\begin{aligned}s &= \sigma + \omega j = -\zeta \omega_n + \omega_n \sqrt{1 - \zeta^2} j \\&= -\alpha \omega_d + j \omega_d \\&\omega_d = \omega_n \sqrt{1 - \zeta^2} \\&\alpha = \frac{\zeta}{\sqrt{1 - \zeta^2}} = \text{Constant}\end{aligned}$$

The mapping of this line to the z-plane yields

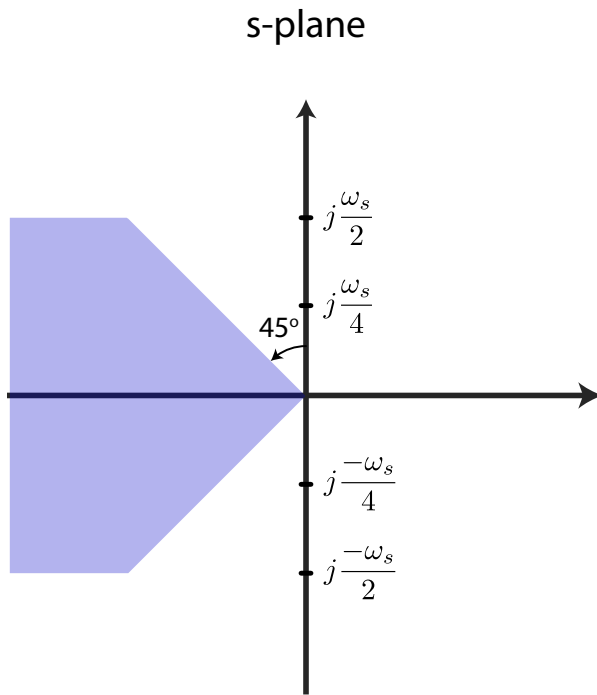
$$\begin{aligned}z &= e^{-\alpha \omega_d T + j T \omega_d} = e^{-\alpha \omega_d T} e^{j \omega_d T} \\z &= e^{-2\pi \alpha \frac{\omega_d}{\omega_s}} e^{j 2\pi \frac{\omega_d}{\omega_s}} \\|z| &= e^{-2\pi \alpha \frac{\omega_d}{\omega_s}} \\&\angle z = 2\pi \frac{\omega_d}{\omega_s}\end{aligned}$$

The curve in z-plane corresponds to a spiral shape as seen in Figure below.

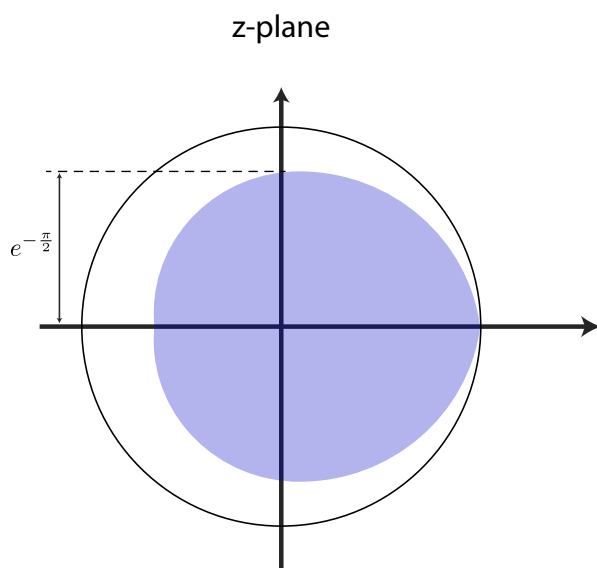


Note that for real systems we need to have also complex conjugates of both the line in s-plane and spiral in z-plane.

Example: Find the mapping of the area defined inside s-plane illustrated in Figure below.



Solution: The solution is illustrated in the Figure below



Bilinear Transformation

A very common transformation used for design and analysis of discrete time control systems, digitized filters etc. is the bilinear transformation. It is a 1-1 mapping between complex z-plane and another complex plane \bar{s} which is an “imaginary” s-domain plane.

The bilinear transformation is defined by

$$z = \frac{1 + \frac{T}{2}\bar{s}}{1 - \frac{T}{2}\bar{s}}$$

$$\bar{s} = \frac{2z - 1}{Tz + 1}$$

Let's analyze $|z| < 1$

$$|z| = \left| \frac{1 + \frac{T}{2}\bar{s}}{1 - \frac{T}{2}\bar{s}} \right| = \frac{|1 + \frac{T}{2}\bar{s}|}{|1 - \frac{T}{2}\bar{s}|}$$

$$|z| < 1 \implies \left| 1 + \frac{T}{2}\bar{s} \right| < \left| 1 - \frac{T}{2}\bar{s} \right|$$

Let $\bar{s} = \bar{\sigma} + j\bar{\omega}$

$$\left| 1 + \frac{T}{2}(\bar{\sigma} + j\bar{\omega}) \right| < \left| 1 - \frac{T}{2}(\bar{\sigma} + j\bar{\omega}) \right|$$

$$\left(\frac{T}{2}\bar{\sigma} + 1 \right)^2 + \left(\frac{T}{2}\bar{\omega} \right)^2 < \left(\frac{T}{2}\bar{\sigma} - 1 \right)^2 + \left(\frac{T}{2}\bar{\omega} \right)^2$$

$$\left(\frac{T}{2}\bar{\sigma} + 1 \right)^2 < \left(\frac{T}{2}\bar{\sigma} - 1 \right)^2 \implies \bar{\sigma} < 0$$

In other words we have the following relation

$$|z| < 1 \iff \operatorname{Re}\{\bar{s}\} < 0$$

which imples that tha area inside unit circle of z-plane (stable region) is mapped to whole open left half plane of \bar{s} -plane.

Now let's consider the mapping of unit-cirlce on z-plane onto the \bar{s} -plane.

$$|z| = 1 \implies \left(\frac{T}{2}\bar{\sigma} + 1 \right)^2 = \left(\frac{T}{2}\bar{\sigma} - 1 \right)^2 \implies \bar{\sigma} = 0$$

which imples that points on the unit circle are mapped to the imaginary axis on the \bar{s} -plane. Now let's analyze this mapping further:

$$|z| = 1 \implies z = e^{j\omega_d}, \omega_d \in [-\pi, \pi]$$

$$\bar{s} = \frac{2e^{j\omega_d} - 1}{T(e^{j\omega_d} + 1)} = \frac{2(e^{j\omega_d} - 1)(e^{-j\omega_d} + 1)}{T(e^{j\omega_d} + 1)(e^{-j\omega_d} + 1)} = j\frac{2}{T} \frac{\sin \omega_d}{1 + \cos \omega_d} = j\frac{2}{T} \frac{\sin(\omega_d/2)}{\cos(\omega_d/2)}$$

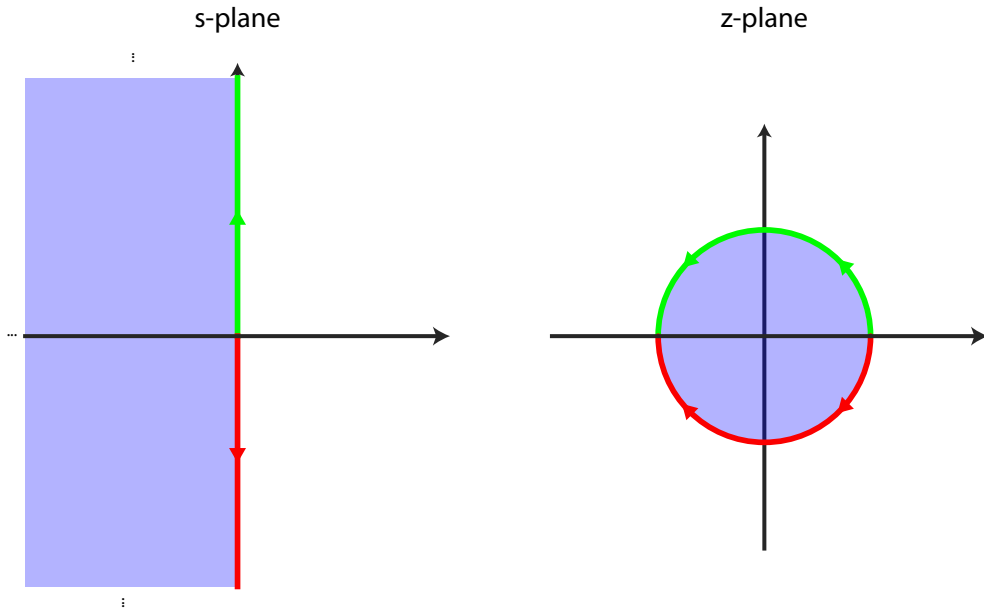
$$\bar{\omega} = \frac{2}{T} \tan(\omega_d/2)$$

where $\bar{\omega}$ is the artificial frequency of the artificial CT system. If we analyze the frequency mapping we can easily see that

$$\omega_d : 0 \rightarrow \pi \implies \bar{\omega} : 0 \rightarrow \infty$$

$$\omega_d : 0 \rightarrow -\pi \implies \bar{\omega} : 0 \rightarrow -\infty$$

Bilinear transformation and its basic mapping properties are illustrated in the Figure below.



Blue transparent region corresponds to open left half plane in \bar{s} -plane and area inside the unit circle in z-plane. Red and green lines/curves illustrate the frequency paths in the respected planes.

Let's analyze the behavior of the frequency mapping around $\omega_d = 0$

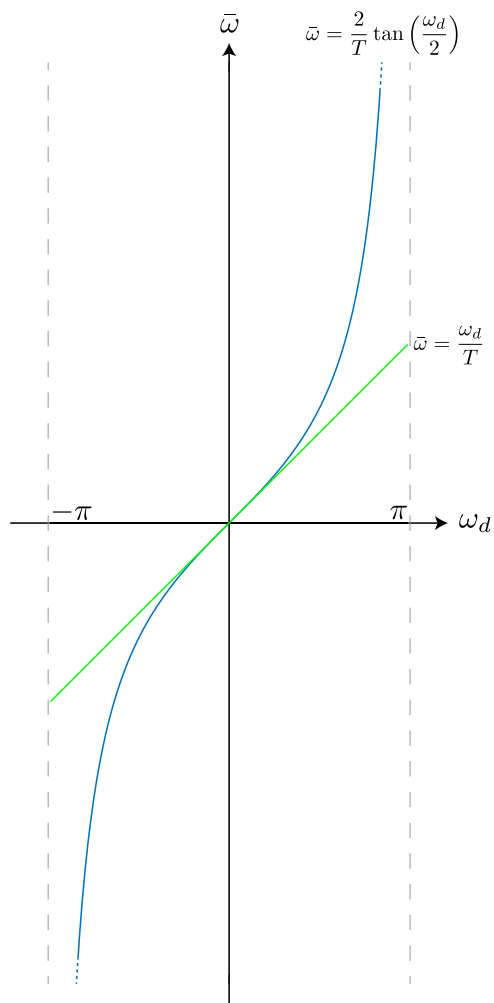
$$\bar{\omega} \approx \left[\frac{d\bar{\omega}}{d\omega_d} \right]_{\omega_d=0} \omega_d = \omega_d/T$$

$$\bar{\omega} \approx \omega_c$$

where $\bar{\omega}$, ω_d , and ω_c are the artificial CT-frequency, frequency in DT domain, and actual frequency in CT domain respectively. The most important relation is that at low frequencies $\bar{\omega} \approx \omega_c$.

In this linear region, the bilinear transformation behaves nicely and we can roughly say that $G(s) \approx G(\bar{s})$. This means that bilinear transformation can be effectively used for design of control systems, or measuring relative performance metrics for the system of interest. However, as ω_d increases there is a highly non-linear frequency wrapping (compression) effect which can make both the design and analysis challenging and sometimes even meaningless.

The Figure below illustrates the relation between ω_d and ω as well as the linear approximation.



Lecture 8

Lecturer: Asst. Prof. M. Mert Ankarali

Stability of Discrete Time Control Systems

For an LTI discrete time dynamical system which can be represented with a rational transfer function, closed loop poles determine the stability characteristics of the system.

- If all poles of the system are located strictly inside the unit-circle then the system is **(asymptotically) stable**. Asymptotically stable systems are also **BIBO stable**.
- If there exist some *simple* (non-repeated) poles on the unit circle and all remaining poles are located inside the unit circle, then the system is **critically/marginally stable**. Note that critically/marginally stable systems are **BIBO unstable**.
- If there exist at least one repeated pole on the unit circle, then the system is **unstable**, of course also **BIBO unstable**.
- If there exist at least one pole outside of the unit circle, then the system is **unstable**, of course also **BIBO unstable**.

Jury Stability Test

Jury stability test similar to the Routh-Hurwitz in CT systems, can define the stability of a DT system given the characteristic equation which is in the form

$$D(z) = a_0 z^n + a_1 z^{n-1} + \cdots + a_{n-1} z + a_n$$

without loss of generality we will assume that $a_0 > 0$.

First Order: When $n = 1$, $D(z)$ takes the form

$$D(z) = a_0 z + a_1$$

DT System is stable if

$$|a_1| < a_0$$

Second Order: When $n = 2$, $D(z)$ takes the form

$$D(z) = a_0 z^2 + a_1 z + a_2$$

DT System is stable if

$$\begin{aligned} |a_2| &< a_0 \\ D(1) &> 0 \\ D(-1) &> 0 \end{aligned}$$

Third Order: When $n = 3$, $D(z)$ takes the form

$$D(z) = a_0 z^3 + a_1 z^2 + a_2 z + a_3$$

We need to construct the Jury table

| Row | z^0 | z^1 | z^2 | z^3 |
|-----|-------|-------|-------|-------|
| 1 | a_3 | a_2 | a_1 | a_0 |
| 2 | a_0 | a_1 | a_2 | a_3 |
| 3 | b_2 | b_1 | b_0 | |

where

$$b_0 = \begin{vmatrix} a_3 & a_2 \\ a_0 & a_1 \end{vmatrix}, \quad b_1 = \begin{vmatrix} a_3 & a_1 \\ a_0 & a_2 \end{vmatrix}, \quad b_2 = \begin{vmatrix} a_3 & a_0 \\ a_0 & a_3 \end{vmatrix}$$

Then DT system is stable if

$$\begin{aligned} |\mathbf{a}_3| &< a_0 \\ D(1) &> 0 \\ -D(-1) &> 0 \\ |b_2| &> |b_0| \end{aligned}$$

General Case: The jury table for systems with order n has $2n - 3$ rows and it has the form below

| Row | z^0 | z^1 | z^2 | \dots | z^{n-2} | z^{n-1} | z^n |
|----------|-----------|-----------|-----------|---------|-----------|-----------|-------|
| 1 | a_n | a_{n-1} | a_{n-2} | \dots | a_2 | a_1 | a_0 |
| 2 | a_0 | a_1 | a_2 | \dots | a_{n-2} | a_{n-1} | a_n |
| 3 | b_{n-1} | b_{n-2} | b_{n-3} | \dots | b_1 | b_0 | |
| 4 | b_0 | b_1 | b_2 | \dots | b_{n-2} | b_{n-1} | |
| 5 | c_{n-2} | c_{n-3} | c_{n-3} | \dots | c_0 | | |
| 6 | c_0 | c_1 | c_2 | \dots | c_{n-2} | | |
| \vdots | \vdots | | | | | | |
| $2n - 3$ | q_2 | q_1 | q_0 | | | | |

where

$$\begin{aligned} b_k &= \begin{vmatrix} a_n & a_{n-1-k} \\ a_0 & a_{k+1} \end{vmatrix}, \quad k \in \{0, 1, \dots, n-1\} \\ c_k &= \begin{vmatrix} b_n & b_{n-2-k} \\ b_0 & b_{k+1} \end{vmatrix}, \quad k \in \{0, 1, \dots, n-2\} \\ q_k &= \begin{vmatrix} p_3 & p_{2-k} \\ p_0 & p_{k+1} \end{vmatrix}, \quad k \in \{0, 1, 3\} \end{aligned}$$

Then DT system is stable if

$$\begin{aligned} |a_n| &< a_0 \\ D(1) &> 0 \\ (-1)^n D(-1) &> 0 \\ |b_{n-1}| &> |b_0| \\ |c_{n-2}| &> |c_0| \\ &\dots \\ |q_2| &> |q_0| \end{aligned}$$

Example: Using Jury test, find if the following characteristic equation is stable or not

$$G(z) = \frac{0.02z^{-1} + 0.03z^{-2} + 0.02z^{-3}}{1 - 3z^{-1} + 4z^{-2} - 2z^{-3} + 0.5z^{-4}}$$

Solution: This is a 4th order system for which the characteristic equation is

$$\begin{aligned} D(z) &= a_0 z^4 + a_1 z^3 + a_2 z^2 + a_3 z + a_4 \\ &= 1z^4 + -3z^3 + 4z^2 + -2z + 0.5 \end{aligned}$$

Jury table for a $n = 4$ system has the form

| Row | z^0 | z^1 | z^2 | z^3 | z^4 |
|-----|-------|-------|-------|-------|-------|
| 1 | a_4 | a_3 | a_2 | a_1 | a_0 |
| 2 | a_0 | a_1 | a_2 | a_3 | a_4 |
| 3 | b_3 | b_2 | b_1 | b_0 | |
| 4 | b_0 | b_1 | b_2 | b_3 | |
| 5 | c_2 | c_1 | c_0 | | |

Before computing the whole Jury table let's check conditions one-by-one

- Check if $|a_4| < a_0$

$$0.5 < 1 \quad \text{OK}$$

- Check if $D(1) > 0$

$$D(1) = 1 - 3 + 4 - 2 + 0.5 = 0.5 > 0 \quad \text{OK}$$

- Check if $(-1)^4 D(-1) > 0$

$$D(-1) = 1 + 3 + 4 + 2 + 0.5 = 10.5 > 0 \quad \text{OK}$$

- Let's compute b_0 and b_3 and check if $|b_3| > |b_0|$

$$b_0 = \begin{vmatrix} a_4 & a_3 \\ a_0 & a_1 \end{vmatrix} = \begin{vmatrix} 0.5 & -2 \\ 1 & -3 \end{vmatrix} = 0.5$$

$$b_3 = \begin{vmatrix} a_4 & a_0 \\ a_0 & a_4 \end{vmatrix} = \begin{vmatrix} 0.5 & 1 \\ 1 & 0.5 \end{vmatrix} = -0.75$$

$$|b_3| = 0.75 > 0.5 = |b_0| \quad \text{OK}$$

- Let's compute b_1 and b_2

$$b_1 = \begin{vmatrix} a_4 & a_2 \\ a_0 & a_2 \end{vmatrix} = \begin{vmatrix} 0.5 & 4 \\ 1 & 4 \end{vmatrix} = -2$$

$$b_2 = \begin{vmatrix} a_4 & a_1 \\ a_0 & a_3 \end{vmatrix} = \begin{vmatrix} 0.5 & -3 \\ 1 & -2 \end{vmatrix} = 2$$

- Let's compute c_0 and c_2 and check if $|c_2| > |c_0|$

$$c_0 = \begin{vmatrix} b_3 & b_2 \\ b_0 & b_1 \end{vmatrix} = \begin{vmatrix} -0.75 & 2 \\ 0.5 & -2 \end{vmatrix} = 0.5$$

$$c_2 = \begin{vmatrix} b_3 & b_0 \\ b_0 & b_3 \end{vmatrix} = \begin{vmatrix} -0.75 & 0.5 \\ 0.5 & -0.75 \end{vmatrix} = 0.3125$$

$$|c_2| = 0.3125 \not> 0.5 = |c_0| \text{ NOT OK}$$

Final Jury Table is also given below

| Row | z^0 | z^1 | z^2 | z^3 | z^4 |
|-----|----------------|------------|-------------|---------------|-------------|
| 1 | $a_4 = 0.5$ | $a_3 = -2$ | $a_2 = 4$ | $a_1 = -3$ | $a_0 = 1$ |
| 2 | $a_0 = 1$ | $a_1 = -3$ | $a_2 = 4$ | $a_3 = -2$ | $a_4 = 0.5$ |
| 3 | $b_3 = -0.75$ | $b_2 = 2$ | $b_1 = -2$ | $b_0 = 0.5$ | |
| 4 | $b_0 = 0.5$ | $b_1 = -2$ | $b_2 = 2$ | $b_3 = -0.75$ | |
| 5 | $c_2 = 0.3125$ | c_1 | $c_0 = 0.5$ | | |

Bilinear Transformation & Routh-Hurwitz Test

In Lecture 7, we showed that bilinear transformation has a 1-1 mapping between stable regions in z-plane and s-plane, as well as unstable regions in z-plane and s-plane. As a way of testing stability, we can transform the characteristic polynomial using bilinear transformation, then we can apply Routh-Hurwitz test.

Routh-Hurwitz is simpler and easier than the Jury test, however amount of computation needed for transformation generally shadows the relative computational advantage of Routh-Hurwitz.

We know that the bilinear transformation has the form

$$z = \frac{1 + \frac{T}{2}\bar{s}}{1 - \frac{T}{2}\bar{s}}$$

Since we only consider the test of stability, for the sake of simplicity it is reasonable to assume that $T = 2$. Then, the transformation of a general $D(z)$ looks like

$$D(\bar{s}) = D(z)|_{z=\frac{1+\bar{s}}{1-\bar{s}}} = a_0 \left(\frac{1+\bar{s}}{1-\bar{s}} \right)^n + a_1 \left(\frac{1+\bar{s}}{1-\bar{s}} \right)^{n-1} + \cdots + a_{n-1} \left(\frac{1+\bar{s}}{1-\bar{s}} \right) + a_n$$

Then clearing the fractions by multiplying both sides by $(1 - \bar{s})^n$, we obtain

$$Q(\bar{s}) = b_0 \bar{s}^n + b_1 \bar{s}^{n-1} + \cdots + b_{n-1} \bar{s} + b_n$$

Testing the stability on $Q(s)$ using Routh-Hurwitz will yield the stability condition of the original DT system.

Example: Consider the following characteristic equation of a DT system

$$D(z) = (z - 1) * (z - 2) = z^2 - 3z + 2 \quad (8.1)$$

Test the stability (already known) using Bilinear Transformation and Routh-Hurwitz.

Solution:

$$D(\bar{s}) = D(z)|_{z=\frac{1+\bar{s}}{1-\bar{s}}} = \left(\frac{1+\bar{s}}{1-\bar{s}} \right)^2 - 3 \left(\frac{1+\bar{s}}{1-\bar{s}} \right) + 2$$

$$\begin{aligned} Q(\bar{s}) &= (1+\bar{s})^2 - 3(1+\bar{s})(1-\bar{s}) + 2(1-\bar{s})^2 \\ &= (1+2\bar{s}+\bar{s}^2) - 3(1-\bar{s}^2) + 2(1-2\bar{s}+\bar{s}^2) \\ &= 6\bar{s}^2 - 2\bar{s} \end{aligned}$$

This artificial CT system is unstable since one coefficient is negative and one coefficient is equal to zero. It is clear from this example that just for testing stability Bilinear transformation is not very useful.

Lecture 9

Lecturer: Asst. Prof. M. Mert Ankarali

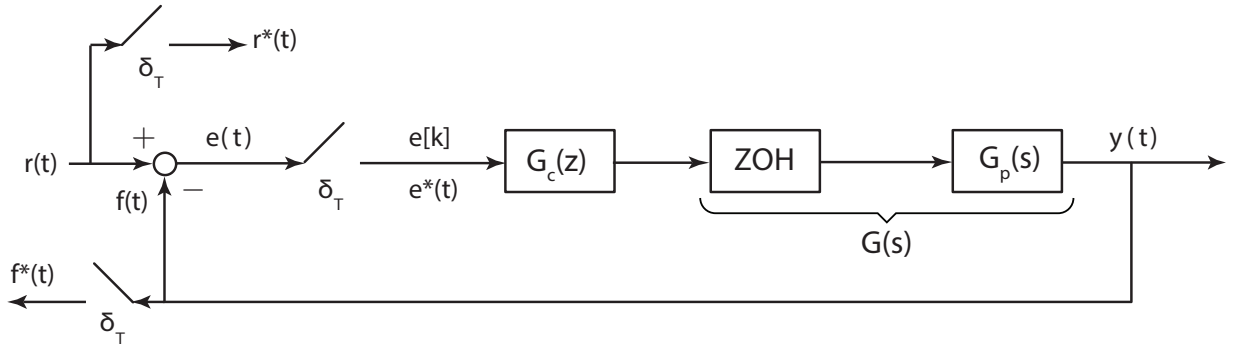
..

Steady-State (DC) Response Analysis

Let's remember the final value theorem. Given a discrete time signal $x[k]$ and its z-transform $X(z)$, if $x[k]$ is convergent sequence final value theorem states that

$$\lim_{k \rightarrow \infty} x[k] = \lim_{z \rightarrow 1} [(1 - z^{-1}) X(z)]$$

$$x_{ss} = \lim_{z \rightarrow 1} \left[\frac{z - 1}{z} X(z) \right]$$



Now let's find the pulse transfer function from the reference signal $r[k]$ to the error signal $e[k]$, to further analyze the steady-state error response.

$$E(z) = R(z) - E(z)(G_c(z)G(z)), \quad \text{where } G(z) = \mathcal{Z}\{G(s)\}$$

$$\frac{E(z)}{R(z)} = \frac{1}{1 + G_c(z)G(z)}$$

Note that $G_c(z)G(z)$ is the pulse transfer function from the error signal $E(z)$ to the signal which is fed to the negative terminal of the main difference operator, i.e. $F(z)$. This transfer function is called feed-forward or open-loop pulse transfer function of the closed-loop digital control system. For this system,

$$\frac{F(z)}{E(z)} = G_{OL} = G_c(z)G(z)$$

Then $E(z)$ can be written as

$$E(z) = R(z) \frac{1}{1 + G_{OL}(z)}$$

It is obvious that first requirement on m steady-state error performance is that closed-loop system have to be stable. Now let's analyze specific but fundamental input scenarios.

Unit-Step Input

We know that $r[k] = u[k]$ and $R(z) = \frac{1}{1-z^{-1}}$ then we have

$$\begin{aligned} e_{ss} &= \lim_{z \rightarrow 1} \left[(1 - z^{-1}) R(z) \frac{1}{1 + G_{OL}(z)} \right] \\ &= \lim_{z \rightarrow 1} \left[(1 - z^{-1}) \frac{1}{1 - z^{-1}} \frac{1}{1 + G_{OL}(z)} \right] \\ e_{ss} &= \frac{1}{1 + \lim_{z \rightarrow 1} G_{OL}(z)} \end{aligned}$$

If the DC gain of the system (also called static error constant) is constant, i.e. $G_{OL}(1) = K_{DC}$ then the steady state error can be computed as

$$e_{ss} = \frac{1}{1 + K_{DC}}$$

It is obvious that

$$\begin{aligned} e_{ss} &\neq 0 \quad \text{if } |K_{DC}| < \infty \\ e_{ss} &\rightarrow 0 \quad \text{if } K_{DC} \rightarrow \infty \end{aligned}$$

Based on these results, we can have the following conclusions

- If $G_{OL}(1) = 0$, then $e_{ss} = 1$. These are **type negative** systems, and we the steady-state error of step response type signals are always 100%.
- If $G_{OL}(1) = K_{DC}$, $0 < |K_{DC}| < \infty$, then $e_{ss} = 1/(1 + K_{DC})$. These are **type 0** systems. We observe a bounded steady-state error and it is possible to reduce the by increasing the static gain constant K_P .
- If $G_{OL}(1) = \infty$, then $e_{ss} = 0$. These are **type positive** systems. The steady-state error is perfectly zero for such systems.

Now let's generalize the *type* of systems. An N *type* closed loop system has the following form of open-loop pulse transfer function

$$\begin{aligned} G_{OL}(z) &= \frac{1}{(z - 1)^N} G_{DC}(z) \\ |G_{DC}(1)| &= K_{DC} \quad \text{where } 0 < |K_{DC}| < \infty \end{aligned}$$

It is easy to see that for unit-step response

- Type $N < 0$: $e_{ss} = 1$ (or $e_{ss} = 100\%$)
- Type $N = 0$: $e_{ss} = 1/(1 + K_{DC})$
- Type $N > 0$: $e_{ss} = 0$

Unit-Ramp Input

We know that $r[k] = ku[k]$ and $R(z) = \frac{z^{-1}}{(1-z^{-1})^2}$ then we have

$$\begin{aligned}
e_{ss} &= \lim_{z \rightarrow 1} \left[(1 - z^{-1}) R(z) \frac{1}{1 + G_{OL}(z)} \right] \\
&= \lim_{z \rightarrow 1} \left[(1 - z^{-1}) \frac{z^{-1}}{(1 - z^{-1})^2} \frac{1}{1 + \frac{1}{(z-1)^N} G_{DC}(z)} \right] \\
&= \lim_{z \rightarrow 1} \left[\frac{1}{z-1} \frac{1}{1 + \frac{1}{(z-1)^N} G_{DC}(z)} \right] \\
&= \lim_{z \rightarrow 1} \left[\frac{1}{(z-1) + \frac{1}{(z-1)^{N-1}} G_{DC}(z)} \right] \\
e_{ss} &= \frac{1}{\lim_{z \rightarrow 1} \left[\frac{1}{(z-1)^{N-1}} G_{DC}(z) \right]}
\end{aligned}$$

Based on this result we can have the following steady-state error conditions for the unit-ramp input based on the type condition of the system

- Type $N < 1$: $e_{ss} \rightarrow \infty$
- Type $N = 1$: $e_{ss} = \frac{1}{K_{DC}}$
- Type $N > 1$: $e_{ss} = 0$

Unit-Quadratic (Acceleration) Input

We know that $r[k] = \frac{1}{2}k^2 u[k]$ and $R(z) = \frac{z^{-1}(1+z^{-1})}{2(1-z^{-1})^3}$ then we have

$$\begin{aligned}
e_{ss} &= \lim_{z \rightarrow 1} \left[(1 - z^{-1}) R(z) \frac{1}{1 + G_{OL}(z)} \right] \\
&= \lim_{z \rightarrow 1} \left[(1 - z^{-1}) \frac{z^{-1}(1+z^{-1})}{2(1-z^{-1})^3} \frac{1}{1 + \frac{1}{(z-1)^N} G_{DC}(z)} \right] \\
&= \lim_{z \rightarrow 1} \left[\frac{(z+1)}{2(z-1)^2} \frac{1}{1 + \frac{1}{(z-1)^N} G_{DC}(z)} \right] \\
&= \lim_{z \rightarrow 1} \left[\frac{(z+1)/2}{(z-1)^2 + \frac{1}{(z-1)^{N-2}} G_{DC}(z)} \right] \\
e_{ss} &= \frac{1}{\lim_{z \rightarrow 1} \left[\frac{1}{(z-1)^{N-2}} G_{DC}(z) \right]}
\end{aligned}$$

- Type $N < 2$: $e_{ss} \rightarrow \infty$
- Type $N = 2$: $e_{ss} = \frac{1}{K_{DC}}$
- Type $N > 2$: $e_{ss} = 0$

Example 1: $G(z) = \frac{z-1}{z-0.5}$ and $G_C(z) = K$. Compute the steady-state erro to unit-step, unit-ramp, a and unit-quadratic inputs.

Solution:

$$G_{OL}(z) = K \frac{z-1}{z-0.5} = \frac{1}{(z-1)^{-1}} \frac{K}{z-0.5}$$

$$G_{DC}(1) = 2K \quad , \text{Type } -1$$

Then the steady-state errors are computed as

- Unit-step: $e_{ss} = 1$
- Unit-ramp: $e_{ss} = \infty$
- Unit-acceleration: $e_{ss} = \infty$

Example 2: $G(z) = \frac{z-1}{z-0.5}$ and $G_C(z) = K \frac{z}{z-1}$. Compute the steady-state error to unit-step, unit-ramp, a and unit-quadratic inputs.

Solution:

$$G_{OL}(z) = \frac{Kz}{z-0.5}$$

$$G_{DC}(1) = 2K \quad , \text{Type } 0$$

Then the steady-state errors are computed as

- Unit-step: $e_{ss} = \frac{1}{1+2K}$
- Unit-ramp: $e_{ss} = \infty$
- Unit-acceleration: $e_{ss} = \infty$

Example 3: $G(z) = \frac{z-1}{z-0.5}$ and $G_C(z) = K \frac{z^2}{(z-1)^2}$. Compute the steady-state erro to unit-step, unit-ramp, a and unit-quadratic inputs.

Solution:

$$G_{OL}(z) = \frac{Kz^2}{(z-1)(z-0.5)} = \frac{1}{z-1} \frac{Kz^2}{z-0.5}$$

$$G_{DC}(1) = 2K \quad , \text{Type } 1$$

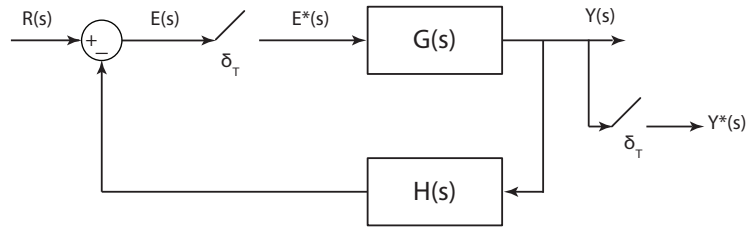
Then the steady-state errors are computed as

- Unit-step: $e_{ss} = 0$
- Unit-ramp: $e_{ss} = \frac{1}{2K}$
- Unit-acceleration: $e_{ss} = \infty$

Open-Loop Transfer Function for Different Topologies

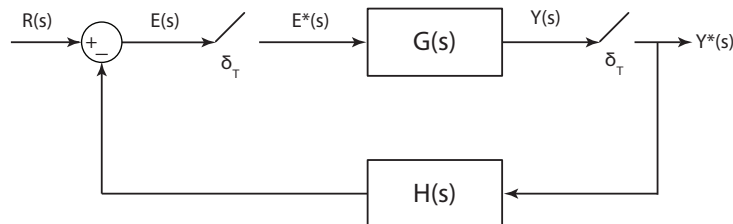
When computing the steady-state error it is important to carefully analyze the topology of the control system.

Compute the $G_{OL}(z)$ for the following system



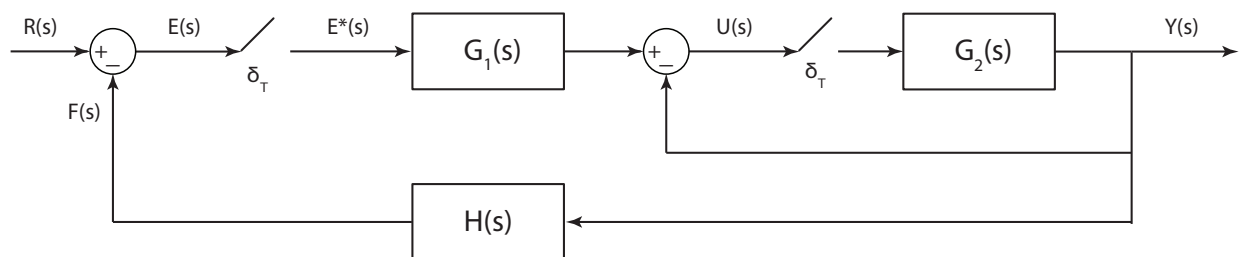
$$\begin{aligned} F(s) &= E^*(s)G(s)H(s) \\ F^*(s) &= E^*(s)[G(s)H(s)]^* = E^*(s)GH^*(s) \\ G_{OL}(z) &= GH(z) \end{aligned}$$

Now let's compute the $G_{OL}(z)$ for the following system



$$\begin{aligned} F(s) &= [E^*(s)G(s)] * H(s) = E^*(s)G^*(s)H(s) \\ F^*(s) &= E^*(s)G^*(s)H^*(s) \\ G_{OL}(z) &= G(z)H(z) \end{aligned}$$

Now let's compute the $G_{OL}(z)$ for the following system



From last week we know that

$$U^*(s) = \frac{G_1^*(s)}{1 + G_2^*(s) + G_1^*(s)GH^*(s)} R^*(s)$$

Then we can

$$\begin{aligned} U(s) &= E^*(s)G_1(s) - U^*(s)G_2(s) \rightarrow U^*(s) = E^*(s)G_1^*(s) - U^*(s)G_2^*(s) \\ U^*(s) &= \frac{G_1^*(s)}{1 + G_2^*(s)} E^*(s) \\ E^*(s) &= \frac{1 + G_2^*(s)}{1 + G_2^*(s) + G_1^*(s)GH^*(s)} R^*(s) \\ \frac{E(z)}{R(z)} &= \frac{1 + G_2(z)}{1 + G_2(z) + G_1(z)GH(z)} \end{aligned}$$

This transfer function form does not (directly) fit to the form we analyzed, i.e. $\frac{E(z)}{R(z)} = \frac{1}{1+G_{OL}(z)}$, so we can not directly used the conditions and formulaes for this form. One way of comuting the steady-state errors is directly applying the final-value theorem.

The other way is we can simply convert the computed pulse transer function $E(z)/R(z)$ such that it fits the form $\frac{E(z)}{R(z)} = \frac{1}{1+G_{OL}(z)}$. If we carefully analyze the transer function we can obtain

$$\begin{aligned} \frac{E(z)}{R(z)} &= \frac{1}{1 + \frac{G_1(z)G_2H(z)}{1+G_2(z)}} \\ G_{OL}(z) &= \frac{G_1(z)G_2H(z)}{1+G_2(z)} \end{aligned}$$

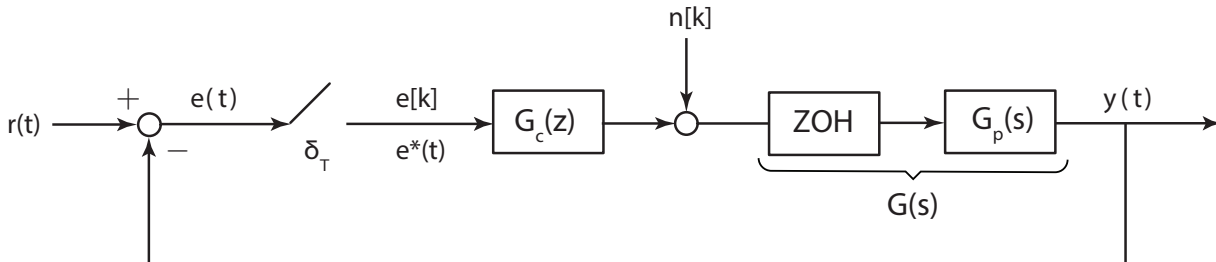
It is also possible to derive $G_{OL}(z)$ via direct computation of $F(z)/E(z)$.

Response to Disturbances

When analyzing response of a system in addition to the desired response to the reference input, it is also important to analyze the response (both steady-state, transient, and frequency) to unwanted disturbances and noises.

Process Disturbance/Uncertainty/Noise

Let's analyze a type of important disturbance on the fundamental discrete-time block diagram topology.



In order to analyze the response to the disturbance $n[k]$, we assume $r[k] = 0$ (which is just fine due to the linearity). Let's first find the pulse transfer function from $N(z)$ to $Y(z)$.

$$Y(z) = (-Y(z)G_c(z) + N(z))G(z)$$

$$\frac{Y(z)}{N(z)} = \frac{G(z)}{1 + G_c(z)G(z)}$$

Technically, we want $\frac{Y(z)}{N(z)} = 0$, while also tracking the reference signal. Since it is not perfectly possible to achieve $\frac{Y(z)}{N(z)} = 0$ while satisfying other constraints, we want $\frac{Y(z)}{N(z)}$ to be “small”. If $|G_C(z)G(z)| \gg 1$ then we have

$$\frac{Y(z)}{N(z)} \approx \frac{1}{G_c(z)}$$

Now let's consider a specific type of disturbance. An important class of process disturbance/uncertainty is in the form of DC bias, i.e. $n(t) = Nu(t)$ and $N(z) = \frac{N}{1-z^{-1}}$. Let's analyze DC steady state response using final value theorem.

$$y_{ss} = \lim_{z \rightarrow 1} [(1 - z^{-1}) Y(z)] = \lim_{z \rightarrow 1} \left[(1 - z^{-1}) N(z) \frac{G(z)}{1 + G_c(z)G(z)} \right]$$

$$= \lim_{z \rightarrow 1} \left[(1 - z^{-1}) \frac{N}{1 - z^{-1}} \frac{G(z)}{1 + G_c(z)G(z)} \right] = \lim_{z \rightarrow 1} \left[N \frac{G(z)}{1 + G_c(z)G(z)} \right]$$

$$= N \frac{\lim_{z \rightarrow 1} G(z)}{1 + \lim_{z \rightarrow 1} G_C(z)G(z)}$$

Let's analyze the steady-state disturbance response

- If plant is a type < 0 system (high pass filter plant) then $G(1) = 0$ and $y_{ss} = 0$.
- If plant is a type 0 system, then

$$y_{ss} = \frac{NG(1)}{1 + G(1)\lim_{z \rightarrow 1} G_C(z)}$$

Now let's analyze the response based on the type of $G_c(z)$

- Type < 0, then

$$y_{ss} = NG(1)$$

In this case, controller has no control on the steady-state disturbance rejection performance.

- Type 0, then

$$y_{ss} = \frac{NG(1)}{1 + G(1)G_C(1)}$$

Obviously in order to “filter” the disturbance we should select a $G_C(z)$ such that $|G_C(1)G(1)| \gg 1$ then

$$y_{ss} = \frac{N}{G_C(1)}$$

Large gain $G_C(z)$ can effectively filter the disturbance (but not completely).

- Type > 0 , then

$$\begin{aligned} y_{ss} &= \frac{NG(1)}{1 + G(1) \lim_{z \rightarrow 1} G_C(z)} \\ &= 0 \end{aligned}$$

Integral action on $G_C(z)$ can perfectly reject the DC disturbance on steady state.

- If plant is a type $m > 0$ then

$$\begin{aligned} y_{ss} &= \frac{N \lim_{z \rightarrow 1} G(z)}{1 + \lim_{z \rightarrow 1} G(z) G_C(z)} \\ \lim_{z \rightarrow 1} G(z) &= \infty \end{aligned}$$

Depending on the type of $G_C(z)$, we can conclude that

- Type < 0 , $y_{ss} = \infty$
- Type 0, $y_{ss} = C$, where $0 < C < \infty$
- Type > 0 , $y_{ss} = 0$

Example 4: $G(z) = \frac{z-1}{z-0.5}$ and $G_C(z) = K$. Compute the steady-state response to a unit step process disturbance/noise.

Solution:

$$y_{ss} = \frac{\lim_{z \rightarrow 1} \frac{z-1}{z-0.5}}{1 + \lim_{z \rightarrow 1} K \frac{z-1}{z-0.5}} = 0$$

Plant perfectly rejects disturbance.

Example 5: $G(z) = \frac{z}{z-0.5}$ and $G_C(z) = K$. Compute the steady-state response to a unit step process disturbance/noise.

Solution:

$$y_{ss} = \frac{\lim_{z \rightarrow 1} \frac{z}{z-0.5}}{1 + \lim_{z \rightarrow 1} K \frac{z}{z-0.5}} = \frac{2}{1 + 2K}$$

Large gain K can be effective solution to reject disturbance

Example 6: $G(z) = \frac{z}{z-0.5}$ and $G_C(z) = K_P + K_I \frac{z}{z-1}$. Compute the steady-state response to a unit step process disturbance/noise.

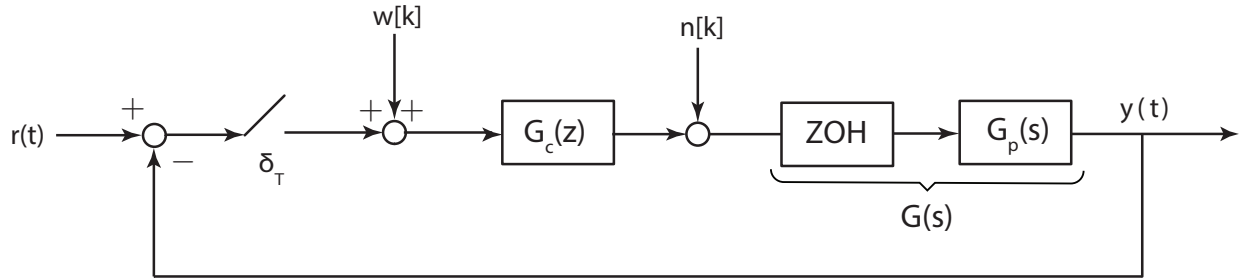
Solution:

$$y_{ss} = \frac{2}{1 + \lim_{z \rightarrow 1} 2 \left(K_P + K_I \frac{z}{z-1} \right)} = 0$$

A PI controller can perfectly reject the DC process disturbance.

Measurement Disturbance/Uncertainty/Noise

Let's analyze a different type of important disturbance on the fundamental discrete-time block diagram topology.



In order to analyze the response to the disturbance $w[k]$, we assume $r[k] = 0$ and $n[k] = 0$

$$\begin{aligned} Y(z) &= (W(z) - Y(z))G_c(z)G(z) \\ \frac{Y(z)}{W(z)} &= \frac{G(z)G_C(z)}{1 + G_c(z)G(z)} \\ &= \frac{G_{OL}(z)}{1 + G_{OL}(z)} \end{aligned}$$

Technically, we want $\frac{Y(z)}{N(z)} = 0$, while also tracking the reference signal. Thus, practically we should design $G_C(z)$ such that $|G_C(z)G(z)| \ll 1$, to eliminate measurement noises/disturbances. (???????)

$$\frac{Y(z)}{N(z)} \approx G_{OL}(z)$$

This “requirement” obviously contradicts with requirements on steady-state tracking error performance and process noise/disturbance rejection performance. Most well known limitation of feedback control systems.

Now let's consider a specific type of measurement noise, i.e. DC measurement bias. $w(t) = Wu(t)$ and $W(z) = \frac{W}{1-z^{-1}}$. Let's analyze DC steady state response using final value theorem.

$$\begin{aligned} y_{ss} &= \lim_{z \rightarrow 1} \left[(1 - z^{-1})R(z) \frac{G_{OL}(z)}{1 + G_{OL}(z)} \right] = \lim_{z \rightarrow 1} \left[(1 - z^{-1}) \frac{W}{1 - z^{-1}} \frac{G_{OL}(z)}{1 + G_{OL}(z)} \right] \\ &= \lim_{z \rightarrow 1} \left[\frac{WG_{OL}(z)}{1 + G_{OL}(z)} \right] \end{aligned}$$

Using the form $G_{OL}(z) = \frac{1}{(z-1)^N} G_{DC}(z)$, y_{ss} takes the form

$$y_{ss} = \lim_{z \rightarrow 1} \left[\frac{WG_{DC}(1)\frac{1}{(z-1)^N}}{1 + G_{DC}(1)\frac{1}{(z-1)^N}} \right]$$

Based on the type of the open-loop transfer function, $G_{OL}(z)$, we can conclude

- Type $N < 0$: $y_{ss} = 0$. Perfect rejection of measurement bias, but we know that this is unacceptable from reference tracking point of view.
- Type $N = 0$

$$y_{ss} = \frac{WG_{DC}(1)}{1 + G_{DC}(1)}$$

It seems that in order to “filter” the measurement bias $G_{DC}(1)$ should be selected very small.

- Type $N > 0$

$$y_{ss} = W$$

The disturbance is directly transferred to the output.

Example 7: $G(z) = \frac{z-1}{z-0.5}$ and $G_C(z) = K$. Compute the steady-state response to a unit step measurement disturbance/noise.

Solution:

$$\begin{aligned} G_{OL}(z) &= K \frac{z-1}{z-0.5} \quad \text{Type -1} \\ y_{ss} &= 0 \end{aligned}$$

Plant perfectly rejects measurement bias.

Example 8: $G(z) = \frac{z}{z-0.5}$ and $G_C(z) = K$. Compute the steady-state response to a unit step process disturbance/noise.

Solution:

$$\begin{aligned} G_{OL}(z) &= K \frac{z}{z-0.5} \quad \text{Type 0} \\ y_{ss} &= \frac{2K}{1+2K} \end{aligned}$$

Small gain K can be effective solution to reject measurement bias.

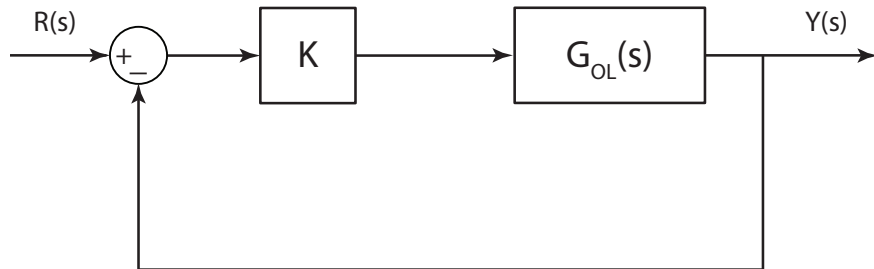
Lecture 10

Lecturer: Asst. Prof. M. Mert Ankarali

..

Root Locus

For continuous time systems the root locus diagram illustrates the location of roots/poles of a closed loop LTI systems, with respect to gain parameter K (can be considered as a P controller). The basic closed-loop topology is used for deriving the root-locus rules, however we know that many different topologies can be reduced to this from.



The closed loop transfer function of this basic control system is

$$\frac{Y(s)}{R(s)} = \frac{KG_{OL}(s)}{1 + KG_{OL}(s)}$$

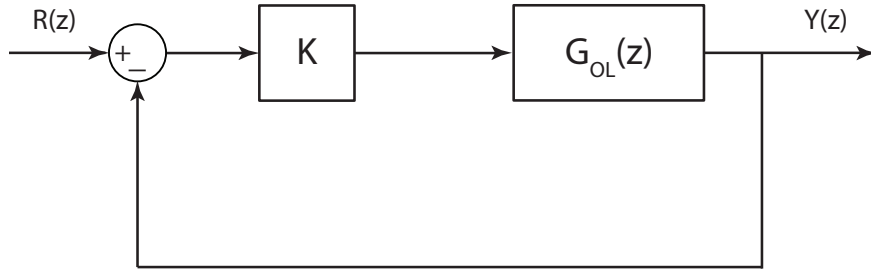
where the poles of the closed loop system are the roots of the characteristic equation

$$1 + KG_{OL}(s) = 0$$

$$1 + K \frac{n(s)}{d(s)} = 0$$

In 302 we learned the rules such that we can derive the qualitative and quantitative structure of root locus paths for **positive** gain K that solves the equation above.

In discrete time systems, similar to the CT case we use the root locus diagram to illustrate the location of roots/poles of a closed loop DT-LTI systems, with respect to a gain parameter K (can be considered as a P controller). The basic discrete-time closed-loop topology is used for deriving the root-locus rules, however we know that many different DT topologies can be reduced to this from.



The closed loop transfer function of this basic control system is

$$\frac{Y(z)}{R(z)} = \frac{KG_{OL}(z)}{1 + KG_{OL}(z)}$$

where the poles of the closed loop system are the roots of the characteristic equation

$$\begin{aligned} 1 + KG_{OL}(z) &= 0 \\ 1 + K \frac{n(z)}{d(z)} &= 0 \end{aligned}$$

I think, it is obvious that fundamental equation that relates the gain K and roots/poles is exactly same for both CT and DT systems. This means that same rules are directly applied for CT systems.

However, even if we have same diagram for CT and DT systems the meaning and interpretation of the diagram is fundamentally different. Because, the effects of pole locations are different in CT and DT systems.

Angle and Magnitude Conditions

Let's analyze the characteristic equation

$$\begin{aligned} KG_{OL}(z) &= -1 \quad \text{,or} \quad K \frac{n(z)}{d(z)} = -1 \\ |KG_{OL}(z)| &= 1 \quad \text{,or} \quad \left| K \frac{n(z)}{d(z)} \right| = 1 \\ \angle[KG_{OL}(z)] &= \pi(2k + 1), \quad k \in \mathbb{Z} \quad \text{,or} \quad \angle\left[K \frac{n(z)}{d(z)} \right] = \pi(2k + 1), \quad k \in \mathbb{Z} \end{aligned}$$

For a given K , z values that satisfy both magnitude and angle conditions are located on the root loci.

Rules and procedure for constructing root loci

- Characteristic equation, zeros and poles of the Open-Loop pulse transfer function.

$$\begin{aligned} 1 + KG_{OL}(z) &= 0 \\ 1 + K \frac{n(z)}{d(z)} &= 0 \\ 1 + K \frac{(z - z_1) \cdots (z - z_M)}{(z - p_1) \cdots (z - p_N)} &= 0 \end{aligned}$$

2. Root loci has N separate branches.
3. Root loci starts from poles of $G_{OL}(z)$ and
 - (a) M branches terminates at the zeros of $G_{OL}(z)$
 - (b) $N - M$ branches terminates at ∞ (implicit zeros of $G_{OL}(z)$)

It is relatively easy to understand this

$$\begin{aligned} d(z) + Kn(z) &= 0 \\ K \rightarrow 0 &\rightarrow d(z) = 0 \\ K \rightarrow \infty &\rightarrow n(z) = 0 \end{aligned}$$

4. Root loci on the real axis determined by open-loop zeros and poles. $z = \sigma \in \mathbb{R}$ then,

$$\begin{aligned} |KG_{OL}(\sigma)| &= 1 \\ \text{Sign}[G_{OL}(\sigma)] &= -1 \end{aligned}$$

We can always find a K that satisfy the magnitude condition, so angle condition will determine which parts of real axis belong to the root locus.

We can first see that complex conjugate zero/pole pairs has no effect, then for the remaining ones we can derive the following condition

$$\text{Sign}[G_{OL}(\sigma)] = \prod_{i=1}^M \text{Sign}[\sigma - z_i] \prod_{j=1}^N \text{Sign}[\sigma - p_j] = -1$$

which means that for ODD number of poles + zeros $\text{Sign}[\sigma - p_i]$ and $\text{Sign}[\sigma - z_i]$ must be negative for satisfying this condition for that particular σ to be on the root-locus. We can summarize the rule as

If the test point σ on real axis has ODD numbers of poles and zeros in its right, then this point is located on the root-locus.

5. Asymptotes

- $N - M$ branches goes to infinity. Thus, there exist $N - M$ many asymptotes
- For large z we can have the following approximation

$$\begin{aligned} K \frac{(z - z_1) \cdots (z - z_M)}{(z - p_1) \cdots (z - p_N)} &\approx \frac{K}{z^{N-M}} \\ \angle \left[\frac{K}{z^{N-M}} \right] &= -(N - M) \angle[z] = \pi(2k + 1), \quad k \in \mathbb{Z} \\ \phi_a &= \frac{\pm \pi(2k + 1)}{N - M}, \quad k \in \{1, \dots, N - M\} \end{aligned}$$

- Real axis intercept σ_a can be computed as

$$\sigma_a = \frac{\sum p_i - \sum z_i}{N - M}$$

This can be derived via a different approximation (see textbook)

6. Breakaway and break-in points on real axis. When z is real $z = \sigma$, $\sigma \in \mathbb{R}$, we can have

$$1 + KG_{OL}(\sigma) = 0 \quad \rightarrow \quad K(\sigma) = \frac{-1}{G_{OL}(\sigma)}$$

Note that break-in and breakaway points corresponds to double roots. Thus, σ_b is a break-away or break-in point if

$$\begin{aligned} \left[\frac{dK(\sigma)}{d\sigma} \right]_{\sigma=\sigma_b} &= 0 \quad \text{or} \quad \left[\frac{dG_{OL}(\sigma)}{d\sigma} \right]_{\sigma=\sigma_b} = 0 \\ K(\sigma) &> 0 \end{aligned}$$

7. Angle of departure (or arrival) from open-loop complex conjugate poles (or to open-loop complex conjugate zeros)

Let's assume that p^* is a complex conjugate pole of $G_{OL}(z)$, then let's define a $P(z)$ such that

$$P^*(z) = (z - p^*)G_{OL}(z)$$

We know that for $K = 0$, the root locus is located at p^* . If we add a very small $K = \delta K$, then pole/root locus moves to $p^* + \delta z$. If we evaluate the phase condition of the root locus on this new "unknown" point

$$\begin{aligned} \angle[KG_{OL}(z)]_{z=p^*+\delta z} &= \pm\pi \\ \angle\left[\frac{P^*(z)}{z - p^*}\right]_{z=p^*+\delta z} &= \pm\pi \\ \angle[P^*(p^* + \delta z)] - \angle[\delta z] &= \pm\pi \\ \theta_d &= \angle[\delta z] = \pm\pi + \angle[P^*(p^*)] \end{aligned}$$

Geometrically speaking, $\angle[P^*(p^*)]$ stands for **# of angles from the zeros to this specific pole – # of angles from all other remaining poles to this specific pole**.

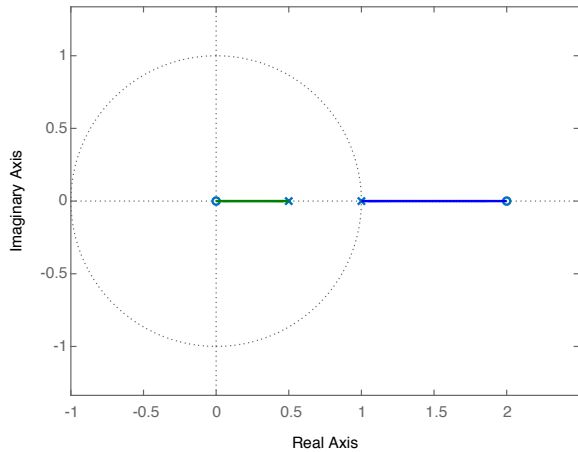
A similar condition can be derived for angle of arrival to complex conjugate zeros.

$$\begin{aligned} \theta_a &= \pm\pi - \angle[P^*(z^*)] \\ P^*(z) &= (z - z^*)G_{OL}(z) \end{aligned}$$

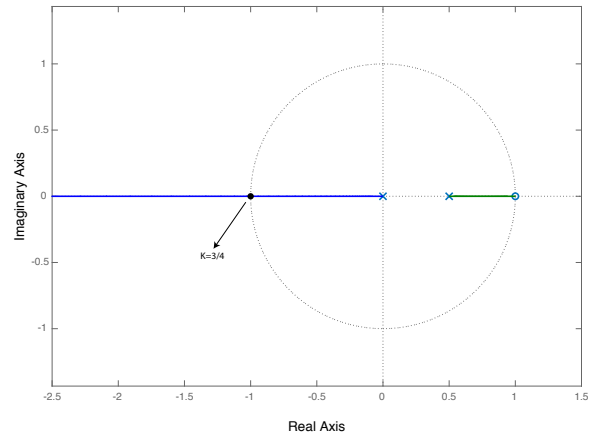
where z^* is a complex conjugate zero of $G_{OL}(z)$.

Examples

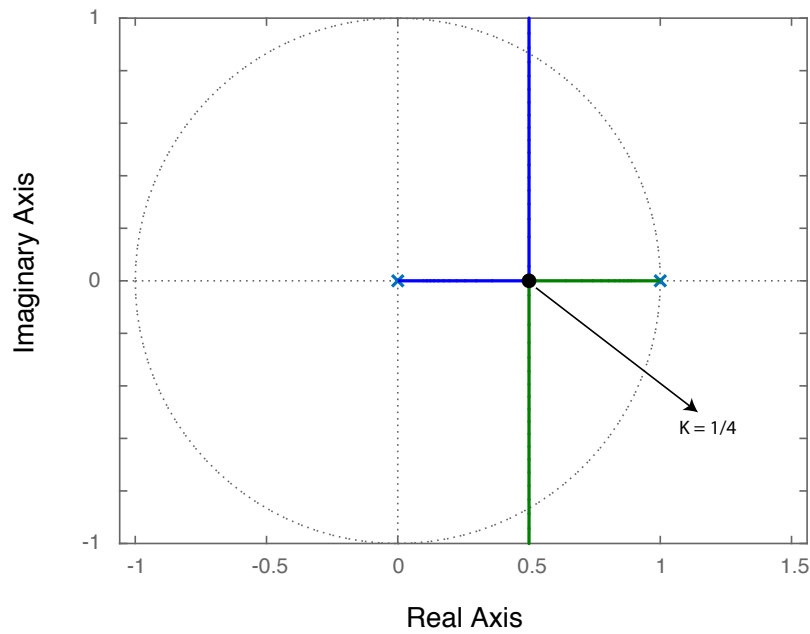
$$G_{OL}(z) = \frac{z(z-2)}{(z-1)(z-0.5)}$$



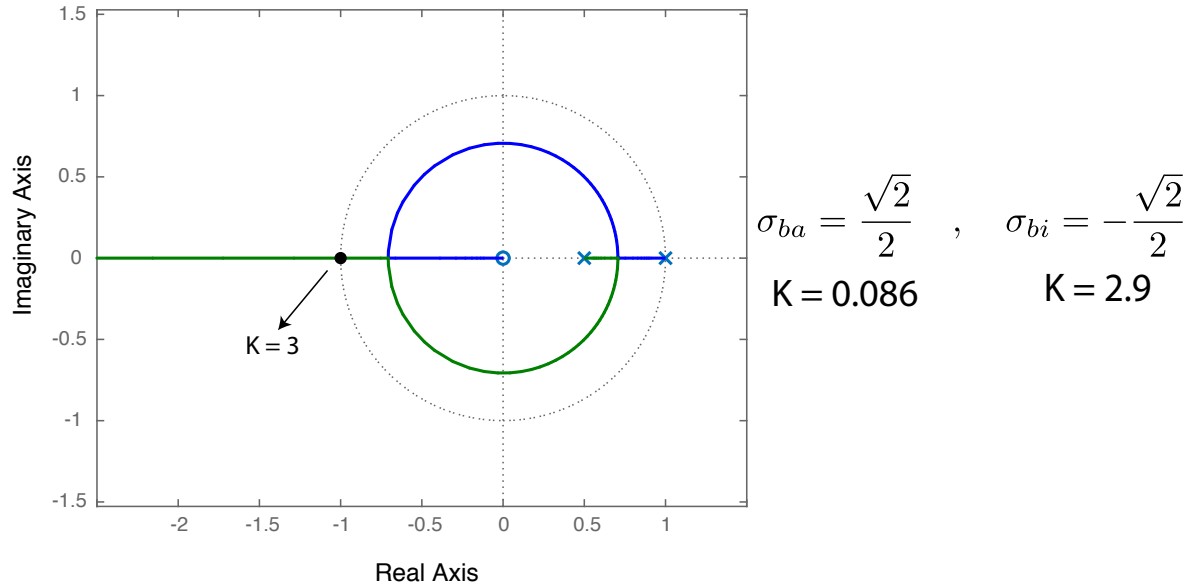
$$G_{OL}(z) = \frac{z-1}{z(z-0.5)}$$



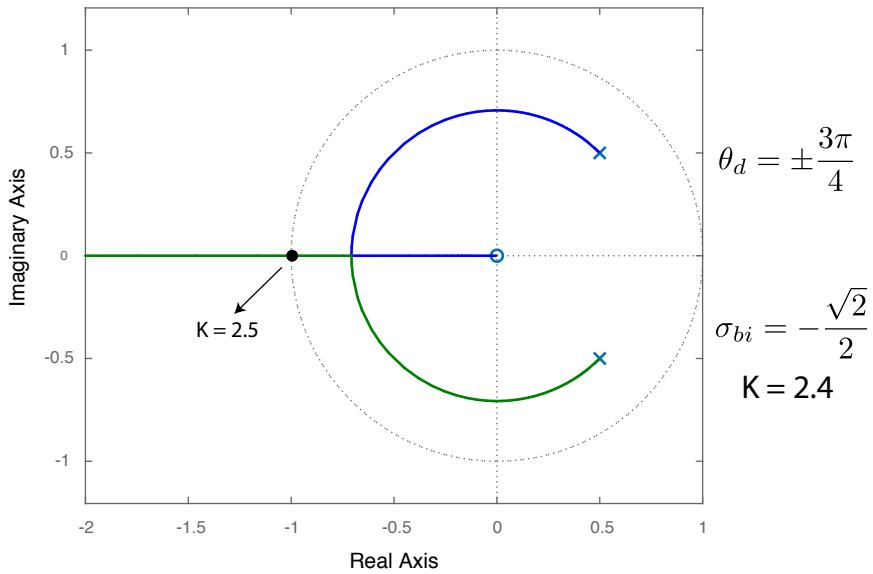
$$G_{OL}(z) = \frac{1}{z(z-1)}$$



$$G_{OL}(z) = \frac{z}{(z - 0.5)(z - 1)}$$

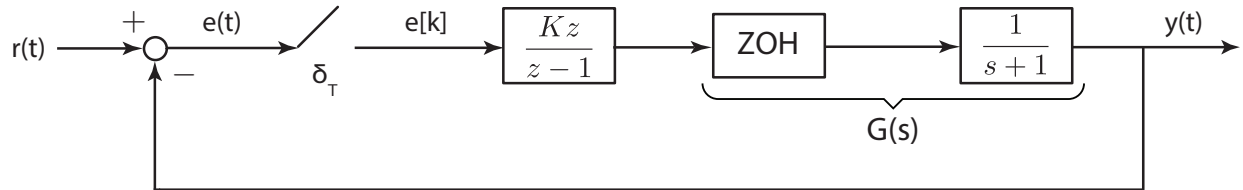


$$G_{OL}(z) = \frac{z}{z^2 - z + 1/2}$$



Root-Locus of Digital Control Systems

Let us draw the root-locus diagrams for the discrete time control system below for $T = 0.5s$, $T = 1s$, and $T = 2s$.



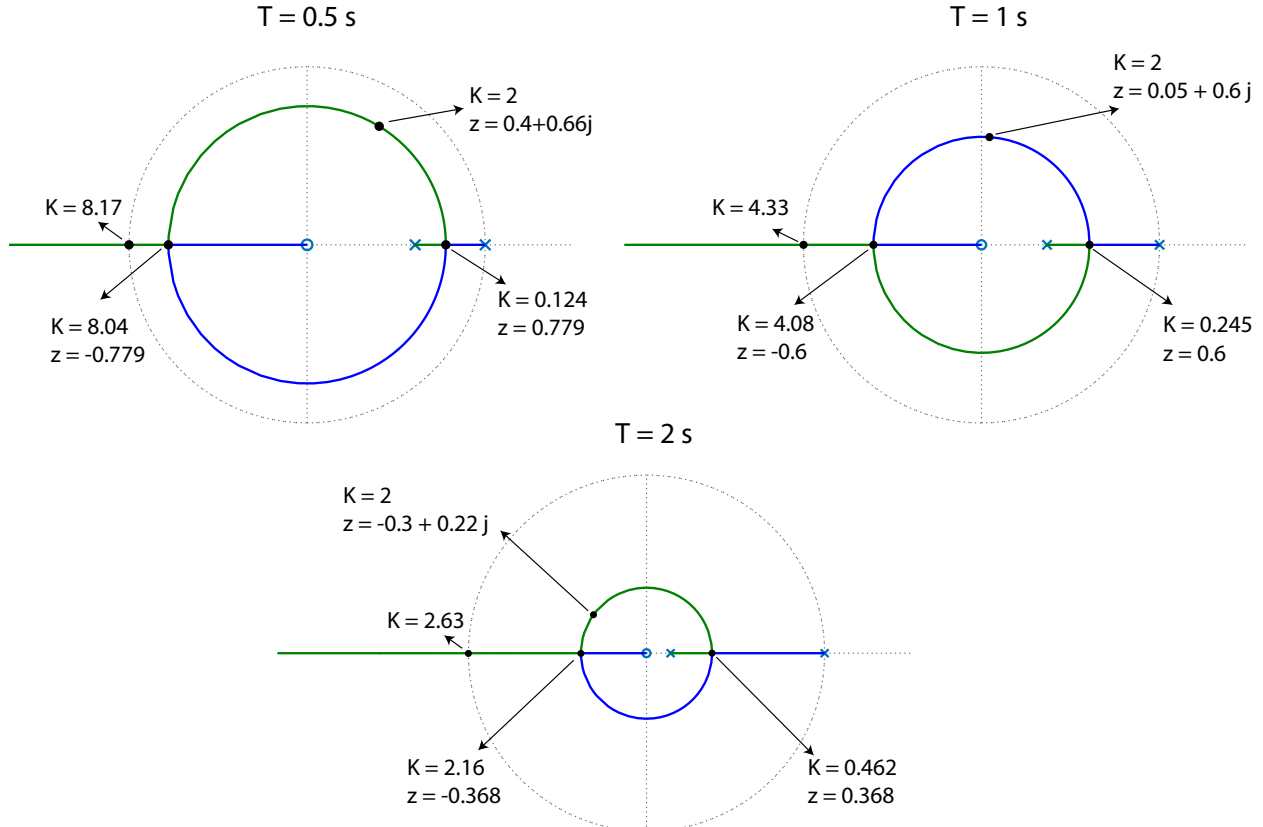
Open-loop pulse transfer functions can be obtained as

$$G_{0.5} = K \cdot 0.3935 \frac{z}{(z-1)(z-0.6065)}$$

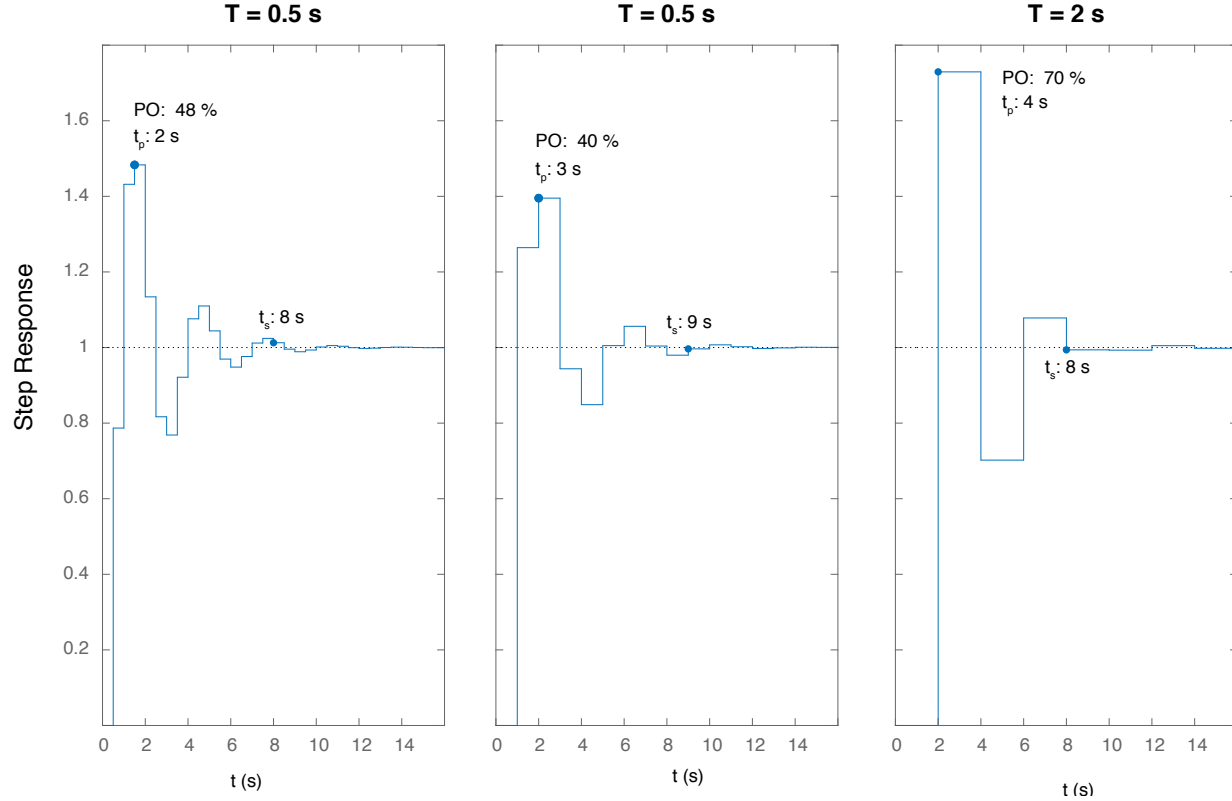
$$G_1 = K \cdot 0.6321 \frac{z}{(z-1)(z-0.3679)}$$

$$G_2 = K \cdot 0.8647 \frac{z}{(z-1)(z-0.1353)}$$

Root-locus plots for all three cases are illustrated in the Figure below.



This Figure below compares DT step responses of all three sampling time cases, where x-axis is the actual time.



If we compare three different responses, we can clearly see that in terms of over-shoot, $T = 2\text{s}$ has the worst performance, whereas $T = 1\text{s}$ seems to be a little better than $T = 0.5\text{s}$. However, if one “draws” the CT-response by simulating the whole hybrid system, he/she can see that the over-shoot for $T = 1\text{s}$ indeed larger than $T = 0.5\text{s}$. Due to the “sampling rate” we can not capture the over-shoot difference clearly between $T = 0.5\text{s}$ and $T = 1\text{s}$. We will talk about it in the next section.

Another similarity between these responses is that settling times of DT-system responses seem to be very close. We know that settling time for a CT-system mainly depends on the real part of the dominant pole, i.e. $\sigma = \text{Re}\{s\}$. Let's compute $\sigma_{0.5}$, σ_1 , and σ_2 by taking into account the $e^{Ts} = z$ mapping.

$$\begin{aligned}\sigma_{0.5} &= \frac{\ln(|z|)}{0.5} \approx -0.5 \\ \sigma_1 &= \frac{\ln(|z|)}{1} \approx -0.5 \\ \sigma_2 &= \frac{\ln(|z|)}{2} \approx -0.5\end{aligned}$$

It can be seen that indeed the real part of the mapped CT pole locations are approximately same for same gain $K = 2$.

Now let's evaluate the steady-state error performances for both sampling times. All three open-loop transfer functions are Type 1 systems and thus for unit step response $e_{ss} = 0$, which is also observable from the step

response plots. Let's compute e_{ss} for unit ramp response.

$$\begin{aligned} e_{0.5} &= \frac{1}{2} \\ e_1 &= \frac{1}{2} \\ e_2 &= \frac{1}{2} \end{aligned}$$

This can give an illusion that they have the same performance. However we evaluated response to the discrete time unit step input which is $r[k] = k[uk]$. However, in order to compare fairly, we need to compute the steady state error to sampled continuous time unit ramp function. $r(t) = t$ & $r(kT) = kT$, thus we have

$$\begin{aligned} r_{0.5}[k] &= 0.5k \\ r_1[k] &= 1k \\ r_2[k] &= 2k \end{aligned}$$

If we re-evaluate the steady-state errors, we obtain

$$\begin{aligned} e_{0.5} &= \frac{1}{4} \\ e_1 &= \frac{1}{2} \\ e_2 &= 1 \end{aligned}$$

Now it is clear that as T increases the steady-state error also increases.

Now let's compare different cases, where each response show a critically damped behavior. Critically damped locations are obtained for the following K values.

$$\begin{aligned} K_{0.5} &= 0.124 \\ K_1 &= 0.245 \\ K_2 &= 0.462 \end{aligned}$$

Now let's compare responses using different specifications

- Obviously no oscillations and 0% overs-shoot for all three cases
- The CT-time mapped pole locations can be computed as

$$\sigma_{0.5} \approx \sigma_1 \approx \sigma_2 \approx -0.5$$

which implies that settling time performance is similar.

- Since all systems are Type 1, the steady-state errors to unit step is zero for all cases.
- If we compute the steady-state errors to sampled CT unit ramp input for all three cases we obtain

$$e_{0.5} \approx e_1 \approx e_2 \approx 4$$

Quite interestingly even the steady-state errors are approximately similar.

This shows that for the specific location where all systems show a critically damped behavior the response performance (stability, overshoot, steady-state error) is quite similar and almost independent on T .

However if one needs to improve the steady-state error performance (to ramp like inputs) obviously lower T (or higher sampling rate) is better both from the perspective of stability and steady-state error performance.

Specs for discrete time pole locations

1. Absolutely we want the poles to be located inside the unit-circle for stability.
2. From the perspective of DT-control systems (CT-systems that are controlled by DT-controllers), we want the frequency of oscillations to be sufficiently smaller than the Nyquist frequency $\omega_s/2$. As a rule of thumb 8-10 samples per cycle are required. Let's assume that require 8 samples per cycle then we have the following condition on z

$$\angle z \in [-\pi/4, \pi/4]$$

3. For a CT system if the system has a dominant second order (or first order) characteristic, then we know that settling time is approximately given by, $T_s = \frac{4}{\sigma}$, where $-\sigma$ is the real part of the CT-pole. Let's assume that the requirement is the settling time of the step response of the system will be less than \bar{T} . Then considering the $z = e^{Ts}$ mapping we have the following condition.

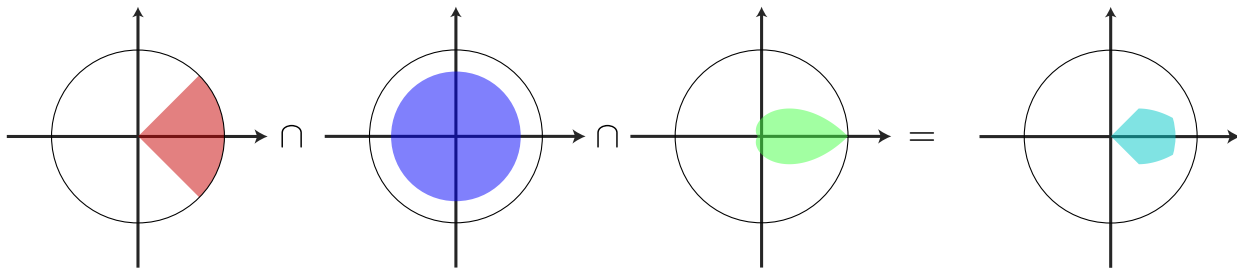
$$\begin{aligned} T_s &\leq \bar{T} \rightarrow \sigma \geq \frac{4}{\bar{T}} \\ |z| &\leq e^{-4\frac{T}{\bar{T}}} \end{aligned}$$

4. Another important requirement for CT systems is the overshoot and damping coefficient. We want damping to be high enough such that overshoot is reasonable. A rule of thumb for damping coefficient is that $\zeta \geq 1/\sqrt{2}$ (However different requirements can also be specified). Based on this we have the following condition on s

$$\begin{aligned} s &= -\alpha\omega_d + \omega_d j \\ \alpha &= \frac{\zeta}{\sqrt{1 - \zeta^2}} \\ \alpha &\geq 1 \end{aligned}$$

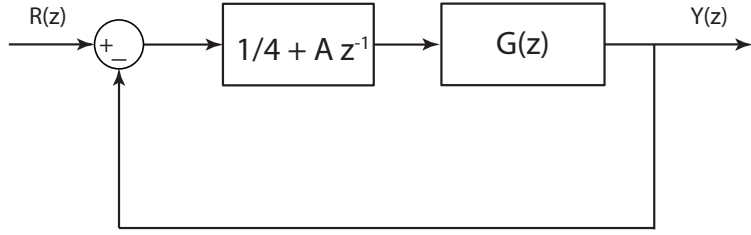
In Lecture 7, we already illustrated the region where $\alpha \geq 1$.

These specs and their combined desired pole location region is illustrated in the Figure below.



Root-locus with respect to different parameters

Let's consider the following purely DT system where plant has a transfer function of $G(z)$ and controller has a first order FIR filter (low-pass) $G_c(z) = 1/4 + Az^{-1}$ form. We wonder the location of closed-loop poles with respect to the parameter A which does not directly fit to the classical form.



Let's first compute the closed-loop PTF and analyze the characteristic equation.

$$\frac{Y(z)}{R(z)} = \frac{(0.25 + Az^{-1}) G(z)}{1 + (0.25 + Az^{-1}) G(z)}$$

$$1 + (0.25 + Az^{-1}) G(z) = 0$$

$$1 + 0.25G(z) + Az^{-1}G(z) = 0$$

If we divide the characteristic equation by $1 + 0.25G(z)$ we obtain

$$1 + A \frac{z^{-1}G(z)}{1 + 0.25G(z)} = 0$$

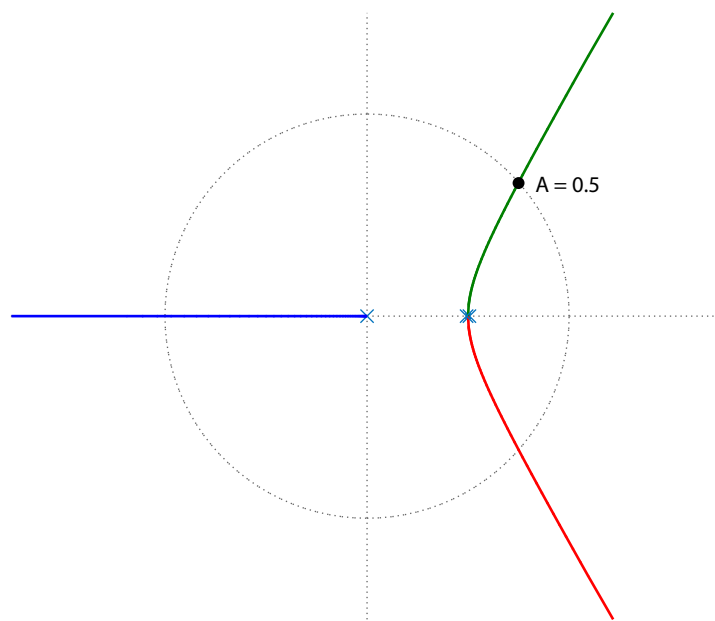
$$1 + A\bar{G}_{OL}(z) = 0$$

Now if we consider as $\bar{G}_{OL}(z)$ as the open-loop transfer function and draw the root-locus then we would derive the dependence of the roots to the parameter A.

Let's assume that $G(z) = \frac{1}{z(z-1)}$. Then for this system, we can compute

$$\begin{aligned}\bar{G}_{OL}(z) &= \frac{z^{-1}G(z)}{1 + 0.25G(z)} = \frac{\frac{1}{z^2(z-1)}}{1 + \frac{0.25}{z(z-1)}} = \frac{\frac{1}{z^2(z-1)}}{\frac{z^2 - z + 0.25}{z(z-1)}} \\ &= \frac{1}{z(z^2 - z + 0.25)}\end{aligned}$$

Root-locus of the system w.r.t parameter A is given below. It can be seen that as A increases, dominant system poles deviates from the origin and eventually becomes unstable at $A = 0.5$. Technically this is a simple low-pass filter which may be inevitable in many closed-loop control systems. However, as we decrease the cut-off frequency (by increasing A) we push the poles towards the unit circle thus making the system less stable.



Lecture 11

Lecturer: Asst. Prof. M. Mert Ankarali

..

Frequency Response in Discrete Time Control Systems

Let's assume $u[k]$, $y[k]$, and $G(z)$ represents the input, output, and transfer function representation of an input-output discrete time system.

In order to characterize frequency response of a discrete system, the test signal is

$$u[k] = e^{j\omega k}$$

which is an artificial complex periodic signal with a DT domain frequency of ω . The z-transform of $u[k]$ takes the form

$$U(z) = \mathcal{Z}\{e^{j\omega k}\} = \frac{z}{z - e^{j\omega}}$$

Response of the system in z-domain is given by

$$Y(z) = G(z)U(z) = G(z) \frac{z}{z - e^{j\omega}}$$

Assuming that $G(z)$ is a rational transfer function we can perform a partial fraction expansion

$$\begin{aligned} Y(z) &= \frac{az}{z - e^{j\omega}} + [\text{terms due to the poles of } G(z)] \\ a &= \lim_{z \rightarrow e^{j\omega}} \left[(z - e^{j\omega}) \frac{Y(z)}{z} \right] = G(e^{j\omega}) \\ Y(z) &= \frac{G(e^{j\omega})z}{z - e^{j\omega}} + [\text{terms due to the poles of } G(z)] \end{aligned}$$

Taking the inverse z-transform yields

$$y(t) = G(e^{j\omega})e^{j\omega k} + \mathcal{Z}^{-1}[\text{terms due to the poles of } G(z)]$$

If we assume that the system is "stable" or system is a part of closed loop system and closed loop behavior is stable then at steady state we have

$$\begin{aligned} y_{ss}[k] &= G(e^{j\omega})e^{j\omega k} \\ &= |G(e^{j\omega})|e^{i\omega k + \angle G(e^{j\omega})} \\ &= M e^{i\omega k + \theta} \end{aligned}$$

In other words complex periodic signal is scaled and phase shifted based on the following operators

$$\begin{aligned} M &= |G(e^{j\omega})| \\ \theta &= \angle G(e^{j\omega}) \end{aligned}$$

It is very easy to show that for a general real time domain signal $u[k] = \sin(\omega k + \phi)$, the output $y[k]$ at steady state is computed via

$$y_{ss}[k] = M \sin(\omega k + \phi + \theta)$$

If there is sampling involved in the system the following relation between DT frequency and CT frequency exists $\omega_d = \omega_c T$

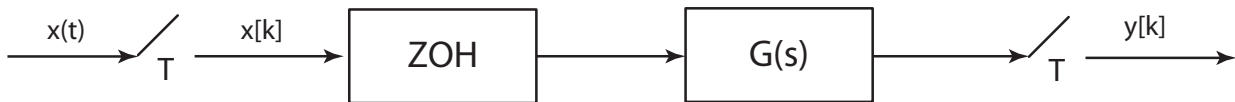
Similar to CT systems we utilize bode plots (or FRF function plots) to analyze DT systems and design filters/controllers. Main difference between CT and DT bode plot is that while the frequency goes to infinity for CT bode plots, for DT systems the frequency goes up-to π rad or $\omega_s/2$ (i.e. Nyquist frequency). Given the bode plot one can extract the magnitude scale and phase difference with respect to any input frequency.

Example: Let's assume that we have the following CT plant transfer function

$$G(s) = \frac{1}{s+1}$$

The pulse transfer function of the following discretized system can be computed as

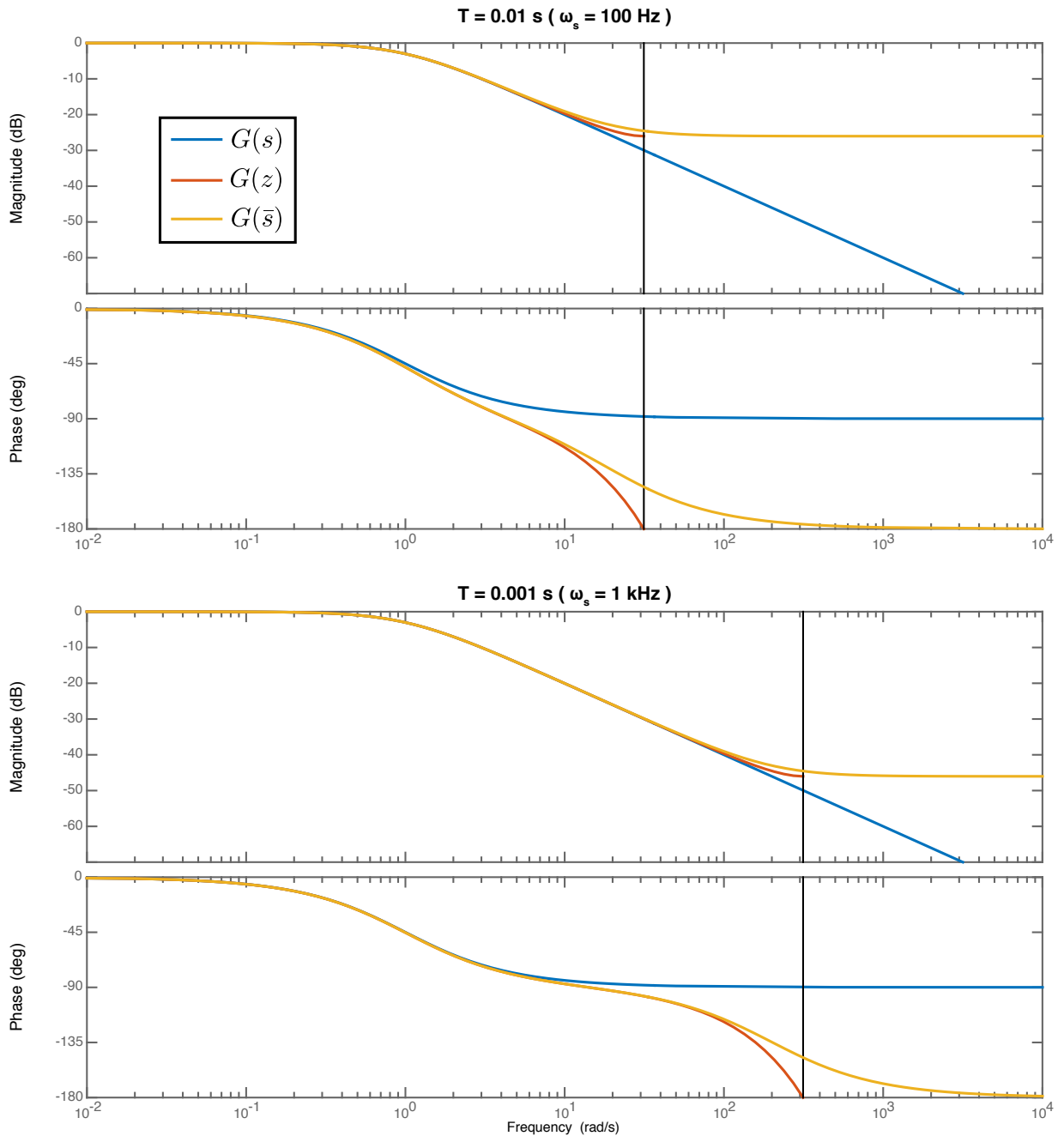
$$G(z) = \mathcal{Z} \left[\frac{1 - e^{-Ts}}{s} \frac{1}{s+1} \right]$$



We can also transform this DT transfer function to an artificial CT form using Bilinear-Tustin transformation.

$$G(\bar{s}) = G(z)|_{z=\frac{1+(T/2)\bar{s}}{1-(T/2)\bar{s}}}$$

Now let's draw the bode plots of $G(s)$, $G(z)$, and $G(\bar{s})$ for both $T = 0.01s$ and $T = 0.001s$.



Phase and Gain Margins

We already know that a binary stability metric is not enough to characterize the system performance and that we need metrics to evaluate how stable the system is and its robustness to perturbations. Using root-locus techniques we talked about some “good” pole regions which provides some specifications about stability and closed-loop performance.

Another common and powerful method is to use gain and phase margins based on the Frequency Response Functions of a closed-loop topology. Phase and gain margins are derived from the Nyquist’s stability criterion and it is relatively easy to compute them from the Bode diagrams.

Gain Margin

The *gain margin*, g_m , of a system is defined as the smallest amount that the open loop gain can be increased before the closed loop system goes unstable. For a system, whose “open-loop” phase response starts from an angle $> -180^\circ$ at $\omega = 0$, the gain margin can be computed based on the smallest frequency where the phase of the loop transfer function $G_{OL}(s)$ is -180° . Let ω_{pc} represent this frequency, called the phase crossover frequency. Then the gain margin for the system is given by

$$g_m = \frac{1}{|G_{OL}(j\omega_{wc})|} \quad \text{or} \quad G_m = -20 \log_{10} |G_{OL}(j\omega_{wc})|$$

where G_m is the gain margin in dB scale.

If the phase response never crosses the -180° line, gain margin is simply ∞ .

Phase Margin

The *phase margin* is the amount of “phase lag” required to reach the (Nyquist) stability limit. Let ω_{gc} be the gain crossover frequency, the smallest frequency where the loop transfer function $G_{OL}(s)$ has unit magnitude. Then for a system for which the gain response at $\omega = 0$ is larger than 1 and gain decreases and eventually crosses the unity gain line, the phase margin is given by

$$\phi_m = \pi + \angle G_{OL}(j\omega_{gc})$$

When the gain and phase plots shows monotonic like behaviors gain and phase margins becomes more meaningful in terms of closed-loop performance.

So far we have only talked about stability margins for a CT control system. Indeed, the Nyquist stability criterion and associated phase and gain margin definitions are almost exactly same, if we consider FRF functions. Let $G_{OL}(z)$ be the open-loop pulse transfer function of a discrete time control system, then the gain and phase margins are computed as

$$g_m = \frac{1}{|G_{OL}(e^{j\omega_{wc}})|} \quad \text{or} \quad G_m = -20 \log_{10} |G_{OL}(e^{j\omega_{wc}})|$$

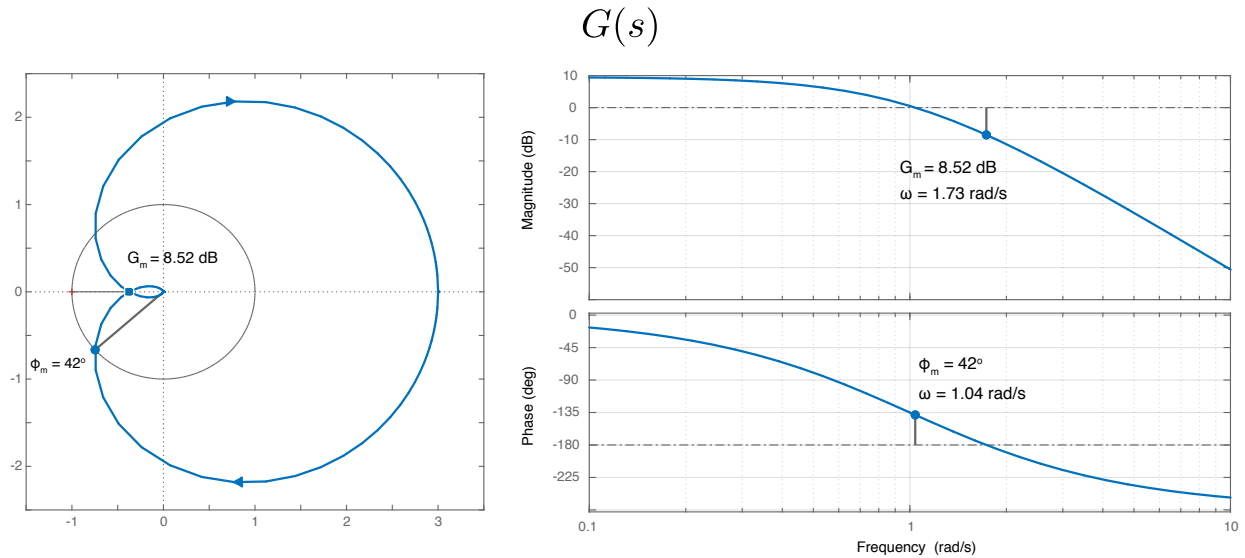
$$\phi_m = \pi + \angle G_{OL}(e^{j\omega_{gc}})$$

where as definitions of gain and phase crossover frequencies are exactly same.

Example: Let's consider a CT plant transfer function

$$G(s) = \frac{3}{(s+1)^3}$$

Nyquist plot, bode diagrams are illustrated in the given Figure below



The phase crossover frequency and gain margin for the CT open-loop transfer function is given below

$$\omega_{pc} = 1.73 \text{ rad/s}$$

$$g_m = \frac{1}{|G(j\omega_{pc})|} = 2.67$$

$$G_m = 8.5dB$$

On the other hand gain crossover frequency and phase margin for $G(s)$ is computed as

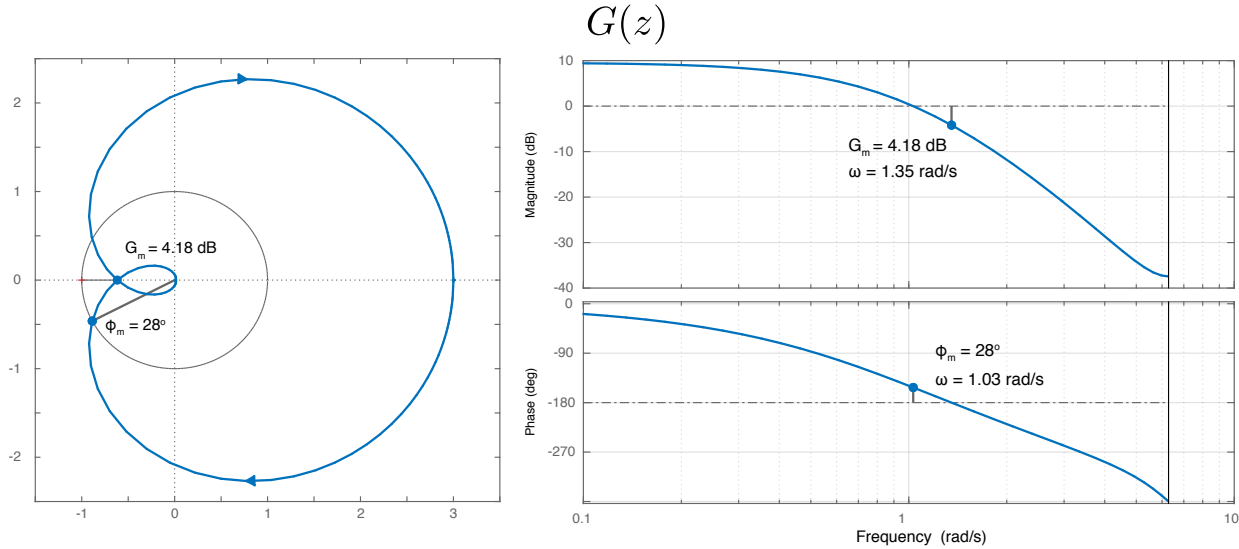
$$\omega_{gc} = 1.04 \text{ rad/s}$$

$$\phi_m = \pi + \angle G(j\omega_{pc}) = 42^\circ$$

Now let's assume that this plant transfer function is controlled via a unity gain digital feedback controller and a ZOH operator, where sampling time is $T = 0.5 \text{ s}$. Open-loop pulse transfer function can be found as

$$G(z) = \left[\frac{1 - e^{-Ts}}{s} G(s) \right]$$

The Nyquist and bode polts for this DT open-loop puls transfer function is illustrated below



Note that instead of DT frequency $\omega_d \in [0, \pi]$, the x-axis illustrates the actual frequency $\omega = \omega_d/T$. It is very easy to associate DT and CT frequencies, and main advantage of actual frequency is that CT and DT versions of bode plots becomes directly comparable.

The phase crossover frequency and gain margin for the DT open-loop transfer function is given below

$$\begin{aligned}\omega_{pc} &= 1.35 \text{ rad/s} \\ g_m &= \frac{1}{|G(e^{j\omega_{pc}T})|} = 1.62 \\ G_m &= 4.18 \text{ dB}\end{aligned}$$

On the other hand gain crossover frequency and phase margin for $G(s)$ is computed as

$$\begin{aligned}\omega_{gc} &= 1.03 \text{ rad/s} \\ \phi_m &= \pi + \angle G(j\omega_{pc}) = 28^\circ\end{aligned}$$

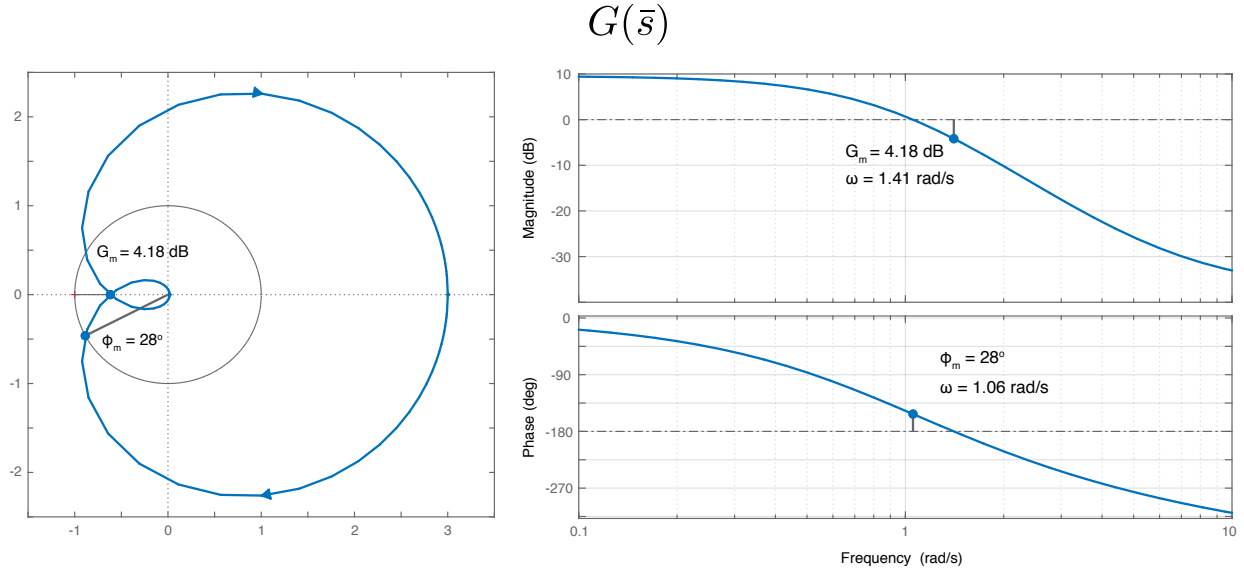
If we compare the CT and DT versions of the same system, we can see that both gain margin and phase margin of the original CT system is better, and we can conclude that discretization reduces the “stability”. Another interesting result is that while there is a significant change in phase-crossover frequency, the change in gain crossover frequency is minimal.

Now let's transfrom the $G(z)$ to a artificial CT system using Bilinear-Tustin transformation:

$$G(\bar{s}) = G(z) \Big|_{z=\frac{1+(T/2)\bar{s}}{1-(T/2)\bar{s}}}$$

We know that the relation between the frequency of this artificial system, $\bar{\omega}$, and frequencies of the actual system and discretized system are given by

$$\bar{\omega} = \frac{2}{T} \tan\left(\frac{\omega_d}{2}\right) = \frac{2}{T} \tan\left(\frac{\omega T}{2}\right)$$



The phase crossover frequency and gain margin for this artificial CT open-loop transfer function is given below

$$\begin{aligned}\omega_{pc} &= 1.41 \text{ rad/s} \\ g_m &= \frac{1}{|G(e^{j\omega_{pc}T})|} = 1.62 \\ G_m &= 4.18 \text{ dB}\end{aligned}$$

On the other hand gain crossover frequency and phase margin for $G(s)$ is computed as

$$\begin{aligned}\omega_{gc} &= 1.06 \text{ rad/s} \\ \phi_m &= \pi + \angle G(j\omega_{pc}) = 28^\circ\end{aligned}$$

If we compare the phase and gain margin and associated crossover frequencies we can see that stability margins of DT and Tustin-Transformed are almost same. It is an expected result, because the core purpose of Tustin transformation is transforming a DT system to a CT form by preserving the stability and other important characteristics.

Tustin transformation has two basic advantages

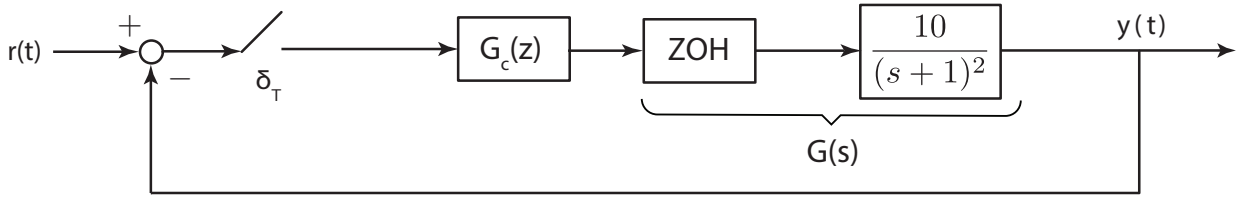
- It “preserves” the stability and robustness characteristics of the digital control system.
- Even though bode plots of DT systems are perfectly valid (and useful), due to periodicity in ω_d the some of the simplicities and advantages of CT bode plots are lost. Since Tustin transformed system is a CT representation, we still can use these simplicities and other advantages.

There two basic disadvantages of Tustin transformation

- It has significant computational costs. However in a computer environment these costs can be negligible.
- If one designs a controller in Tustin form, and then back-transformes the controller in DT form. For some class of controller the quantization effects can become important and deadly.

Lead-Compensator Design for DT Control Systems

Let's consider the DT control system below. Let's assume that $T = 0.1s$



The goal is designing a DT phase-lead compensator such that the Phase-Margin is of the controlled system is in the desired range of $\phi_m \in [50^\circ, 60^\circ]$.

Due to nice properties of CT bode plots, lead-compensator design procedure is handled in the Bilinear-Tustin transformed domain. Below we will summarize the process for the example plant.

1. Compute discretized plant transfer function $G(z)$

$$\begin{aligned} G(z) &= \mathcal{Z} \left[\frac{1 - e^{-Ts}}{s} G_P(s) \right] \\ &= \mathcal{Z} \left[\frac{1 - e^{-Ts}}{s} \frac{10}{(s + 1)^2} \right] \\ &= \frac{0.047z + 0.044}{z^2 - 1.8z + 0.82} \end{aligned}$$

2. Compute the Bilinear-Tustin transformation of $G(z)$

$$\begin{aligned} G(\bar{s}) &= G(z)|_{z=\frac{1+(T/2)\bar{s}}{1-(T/2)\bar{s}}} \\ &= \frac{-0.0008\bar{s}^2 - 0.48\bar{s} + 9.98}{\bar{s}^2 + 2\bar{s} + 0.998} \end{aligned}$$

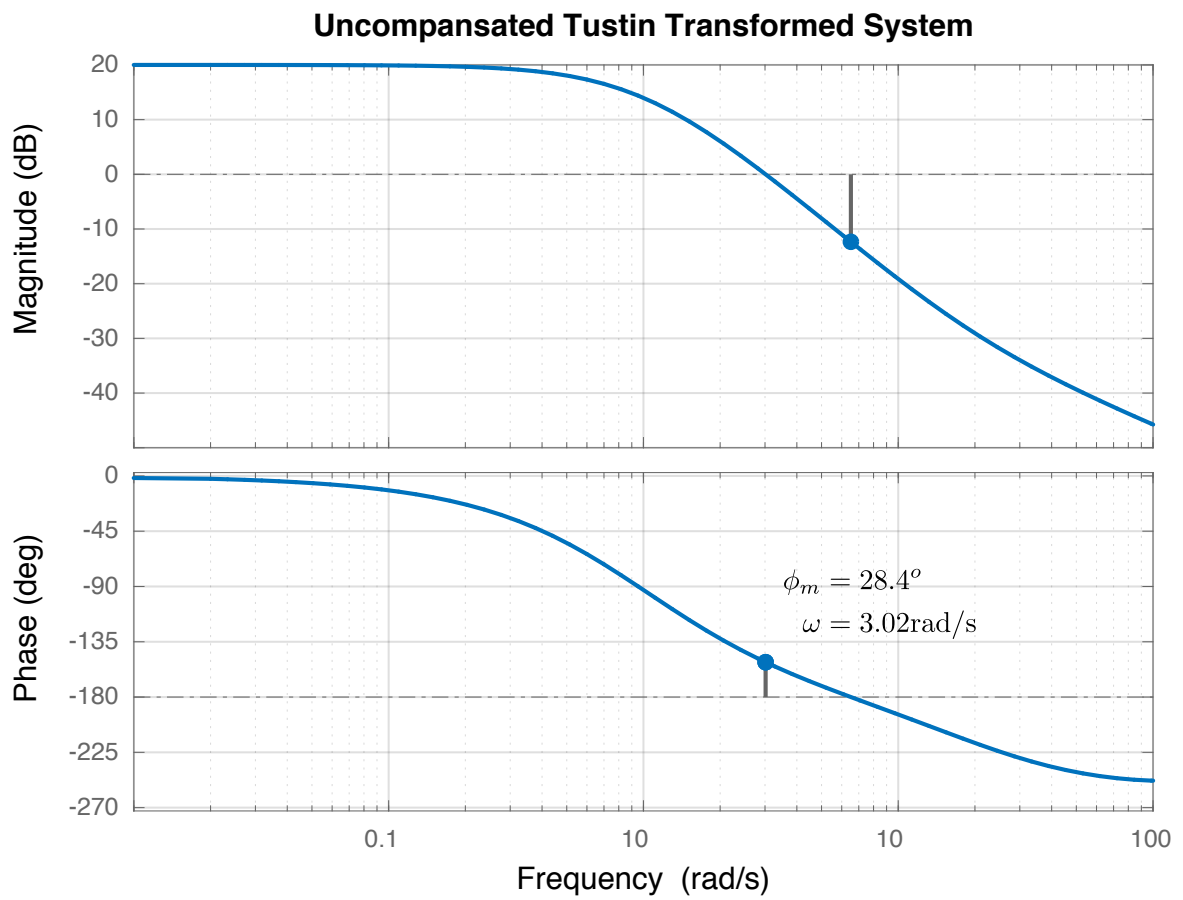
3. Now goal is designing a lead compensator for $G(\bar{s})$. Lead-compensator has the form.

$$G_l(\bar{s}) = K_{\text{lead}} \frac{T_l a \bar{s} + 1}{T_l/a \bar{s} + 1}$$

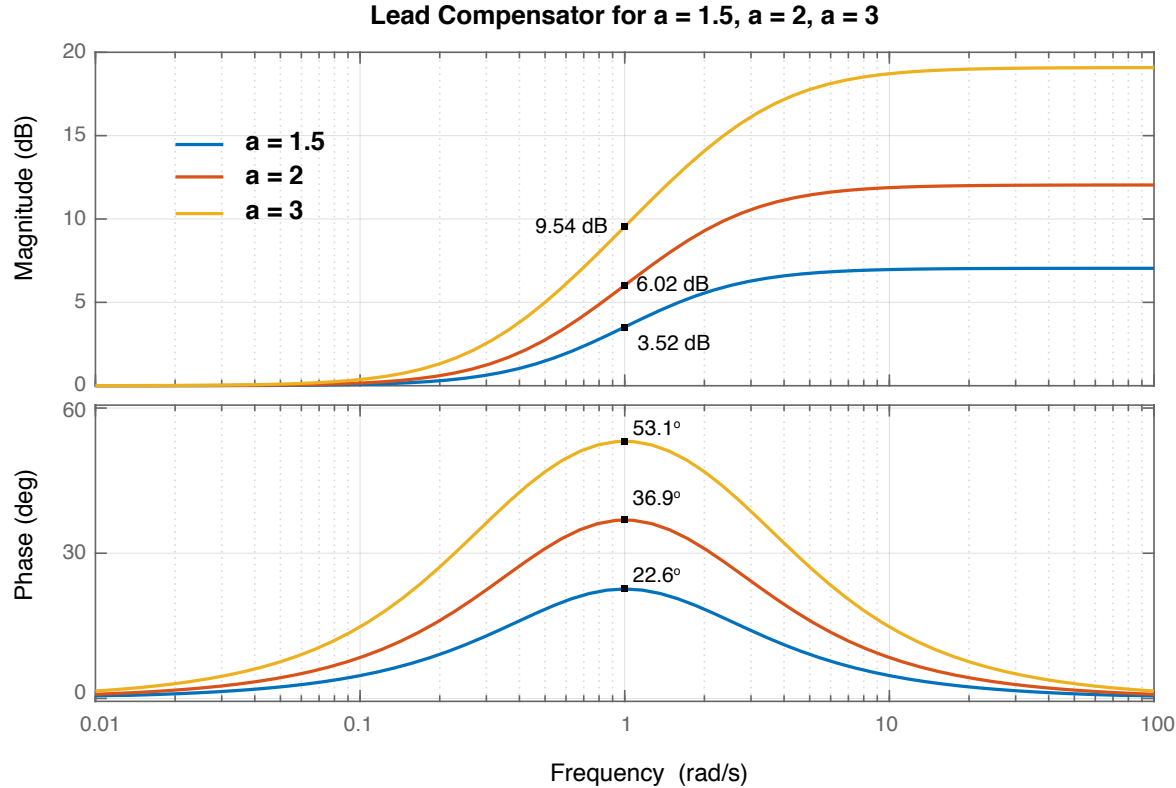
where gain K_l (generally) computed based on steady state requirements. This can be computed either in z-domain or s-bar domain. Let's assume that we are OK with steady-state performance and $K_l = 1$.

4. Compute the ϕ_m of the un-compensated system and find the required $\Delta\phi_m$ such that the compensated system meets the specifications.

$$\begin{aligned} \phi_m &\approx 28^\circ \\ \Delta\phi_m &= [22^\circ, 32^\circ] \end{aligned}$$



5. For $a = 1.5$, $a = 2$, and $a = 3$, bode plots of a phase-lead compensator is illustrated with $T_l = 1$ in the figure below.



It can be seen that ϕ_{max} is larger for large a . ϕ_{max} (or a) can also be computed using the following relation.

$$\sin \phi_{max} = \frac{a^2 - 1}{a^2 + 1}$$

As you remember from EE302, Lead compensator should have a lead angle that is above $\approx 5 - 15^\circ$ the required $\Delta\phi_m$. Based on this we compute/find a . Based on the bode plots, it seems that $a = 2$ may supply the required additional phase-margin. One should see that ϕ_{max} is not affected from the choice of T_l .

6. Now our goal is to compute T_l , where $1/T_l$ corresponds to the center frequency of the compensator. One possible choice is choosing T such that $1/T_l = \bar{\omega}_{gc}$, i.e. gain crossover frequency. However, at center frequency the lead compensator shifts the bode magnitude by

$$G_{center} = 20\log_{10}(1/a)$$

which causes a shift in gain-crossover frequency. For example, for $a = 2$, $G_{center} \approx 6 \text{ dB}$. For this reason, a “better” choice is choosing T such that center frequency of the lead-compensator coincides with the frequency where $|G(j\bar{\omega})|$ crosses $-20 \log_{10}(1/a)$, i.e. we compute T_l such that

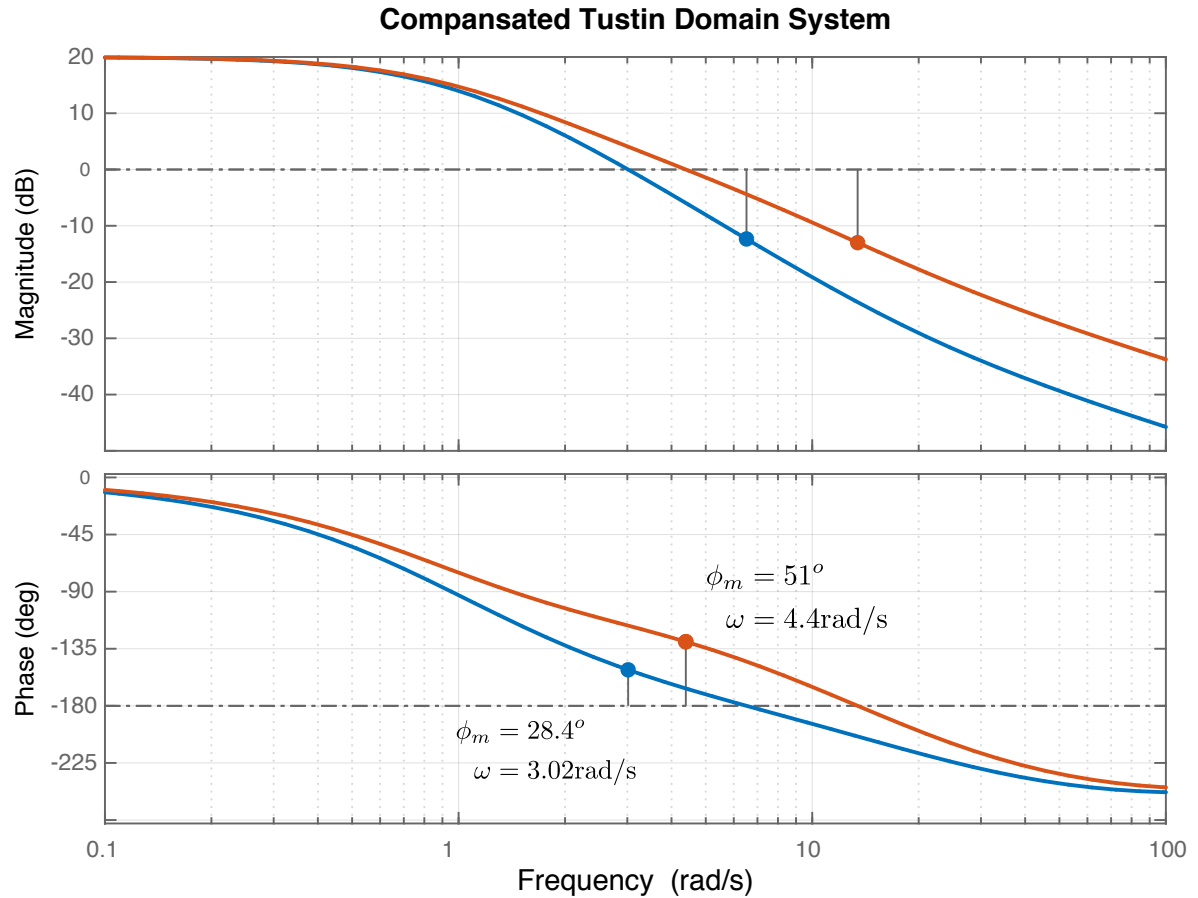
$$|G(j1/T_l)| = -20 \log_{10}(1/a)$$

From the bode plots for $a = 2$, the frequency for which $G(\bar{s})$ crosses the -6 dB line is approximately 4.45 rad/s. Thus we choose $T = 0.225s$. Check if the lead-compensator meets the phase-margin requirement. Otherwise, repeat the process with a higher $\delta\phi$ angle.

In our example, the resultant Tustin domain lead compensator has the form.

$$G_l(\bar{s}) = \frac{0.45s + 1}{0.1125s + 1}$$

The Figure below illiustrates the bode plots of both (tustin domain) compensated and uncompensated systems. Compensated systems has a phase margin of $\phi_m = 51^\circ$ which meets the requirements.

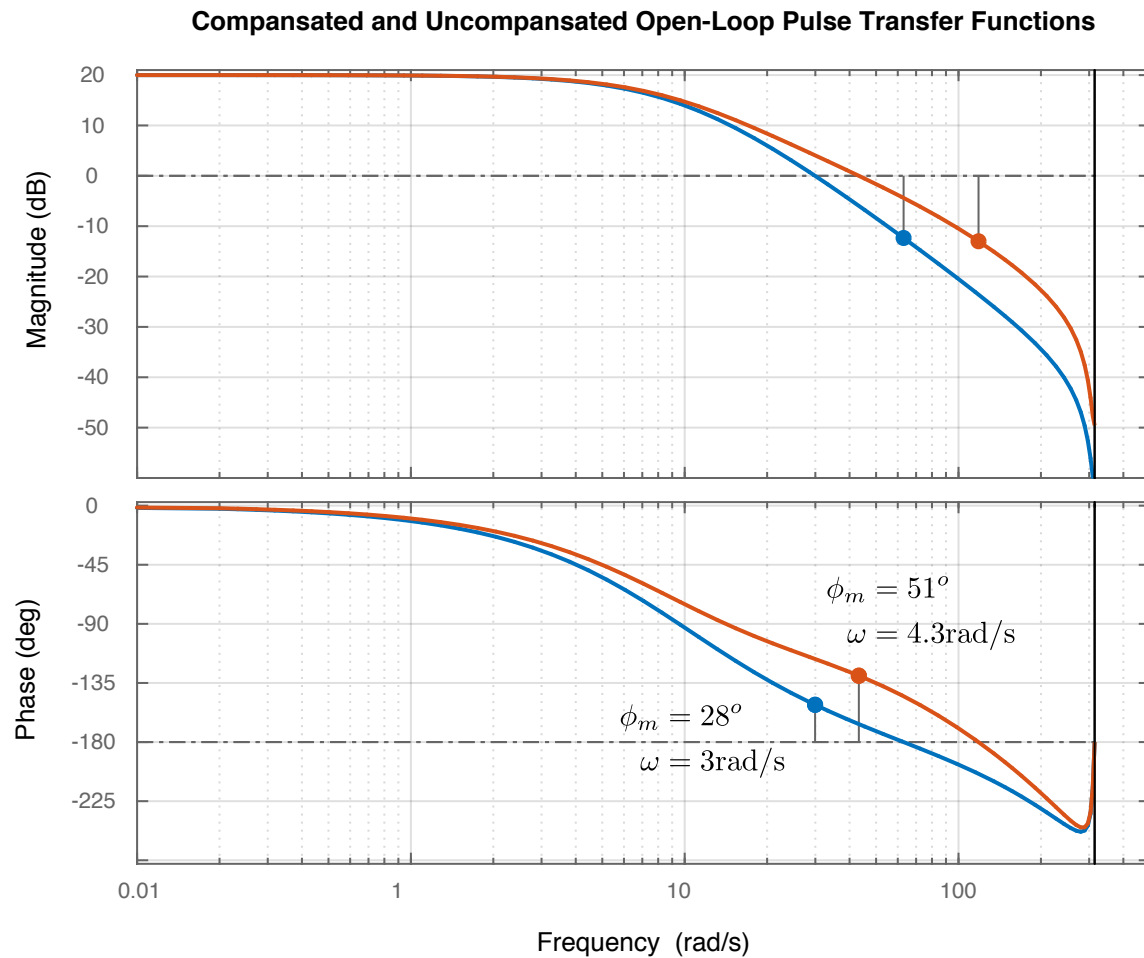


- Transform the \bar{s} -domain lead-compensator to z-domain.

$$G_l(z) = G_l(\bar{s})|_{\bar{s}=\frac{2}{T}\frac{z-1}{z+1}}$$

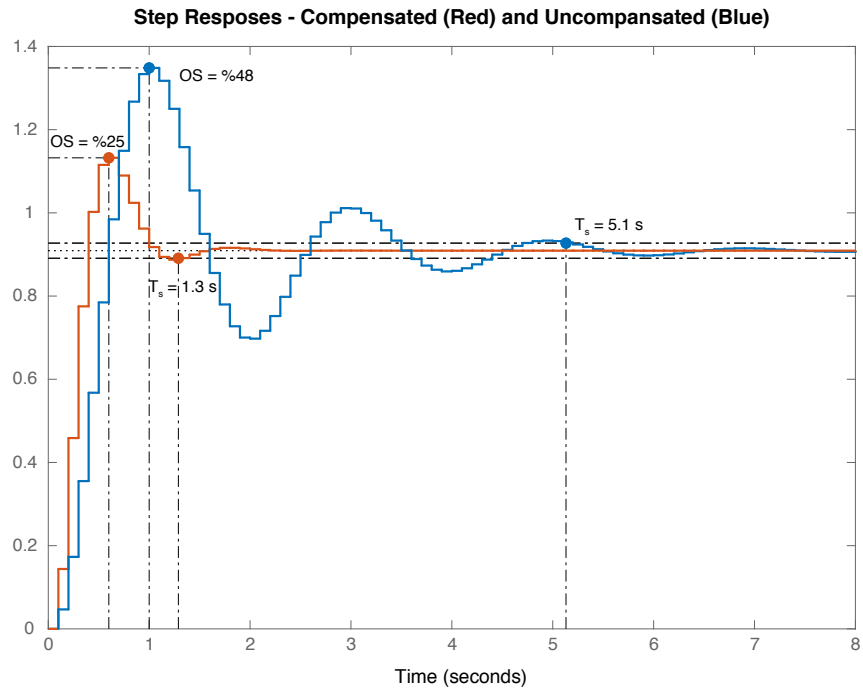
$$G_l(z) = \frac{3.08z - 2.46}{z - 0.385}$$

- Check if the discrete-time compensator meets the the phse-margin requirments.



It can be seen that the designed compensator in z-domain also meets the phase-margin specifications.

In Figure below, we compare the closed-loop step responses of both uncompensated and compensated pulse transfer functions.



Lecture 12

Lecturer: Asst. Prof. M. Mert Ankarali

State-Space Representation of DT Systems

State-space representation of a (causal & finite dimensional) LTI CT system is given by

$$\begin{aligned} \text{Let } x(t) &\in \mathbb{R}^n, y(t) \in \mathbb{R}^m, u(t) \in \mathbb{R}^r, \\ \dot{x}(t) &= Ax(t) + Bu(t), \\ y(t) &= Cx(t) + Du(t), \\ \text{where } A &\in \mathbb{R}^{n \times n}, B \in \mathbb{R}^{n \times r}, C \in \mathbb{R}^{m \times n}, D \in \mathbb{R}^{m \times r} \end{aligned}$$

State-space representation of a (causal & finite dimensional) LTI DT system is given by

$$\begin{aligned} \text{Let } x[k] &\in \mathbb{R}^n, y[k] \in \mathbb{R}^m, u[k] \in \mathbb{R}^r, \\ x[k+1] &= Gx[k] + Hu[k], \\ y[k] &= Cx[k] + Du[k], \\ \text{where } G &\in \mathbb{R}^{n \times n}, H \in \mathbb{R}^{n \times r}, C \in \mathbb{R}^{m \times n}, D \in \mathbb{R}^{m \times r} \end{aligned}$$

Depending on the values of m and r we have

- $m = r = 1$, the system represents a SISO system
- $m > 1, r < 1$, the system represents a MIMO system
- $m = 1, r > 1$, the system represents a MISO system
- $m > 1, r = 1$, the system represents a SIMO system

for both CT and DT cases.

State property of CT state-space models: Given the initial time, t_0 and state $x(t_0)$ and input $u(t)$ for $t_0 \leq t < t_f$ (with t_0 & t_f arbitrary), we can compute the output $y(t)$ for $t_0 \leq t \leq t_f$ and the state $x(t)$ for $t_0 \leq t \leq t_f$.

State property of DT state-space models: Given the state vector $x[k]$ and input $u[k]$ at an arbitrary time k , we can compute the present output, $y[k]$, and next state $x[k+1]$.

Note that both definitions are not limited to LTI state-space models. Nonlinear and time-varying state-space models also are based on this definition.

When a state-space representation includes minimum number of state variables, the representation is called minimal.

Canonical State-Space Realizations of (SISO) DT Systems

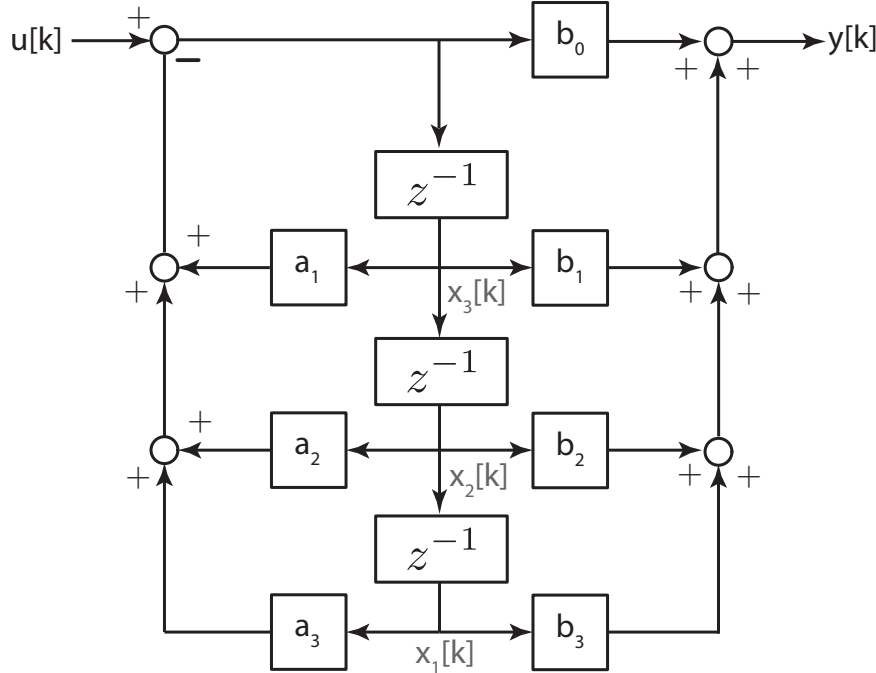
Reachable/Controllable Canonical Form

For the sake of clarity let's assume that the system that we would like to represent is a third order DT system with the following difference equation and transfer function

$$y[k] = -a_1 y[k-1] - a_2 y[k-2] - a_3 y[k-3] + b_0 x[k] + b_1 x[k-1] + b_2 x[k-2] + b_3 x[k-3]$$

$$Y(z) = \frac{b_0 + b_1 z^{-1} + b_2 z^{-2} + b_3 z^{-3}}{1 + a_1 z^{-1} + a_2 z^{-2} + a_3 z^{-3}} X(z)$$

We know that following block diagram realizes this system structure with minimum number of delay elements and it is a canonical realization. Delay operation is directly related with state and state evolution concept.



If we label the signals as given in the Figure, state evolution equations can be derived as

$$X_1(z) = X_2(z)z^{-1} \rightarrow x_1[k+1] = x_2[k]$$

$$X_2(z) = X_3(z)z^{-1} \rightarrow x_2[k+1] = x_3[k]$$

$$X_3(z) = (U(z) - (X_1(z)a_3 + X_2(z)a_2 + X_3(z)a_1))z^{-1} \rightarrow x_3[k+1] = u[k] + x_1[k](-a_3) + x_2[k](-a_2) + x_3[k](-a_1)$$

where as output equation can be derived as

$$\begin{aligned} y[k] &= b_1 x_3[k] + b_2 x_2[k] + b_3 x_1[k] b_0 u[k] - b_0 (a_1 x_3[k] + a_2 x_2[k] + a_3 x_1[k]) \\ &= b_0 u[k] + (b_3 - b_0 a_3)x_1[k] + +(b_2 - b_0 a_2)x_2[k] + +(b_1 - b_0 a_1)x_3[k] \end{aligned}$$

If we gather these equations, we can obtain the state space form

$$\begin{aligned}\mathbf{x}[k+1] &= \begin{bmatrix} 0 & 1 & 0 \\ 0 & 0 & 1 \\ -a_3 & -a_2 & -a_1 \end{bmatrix} \mathbf{x}[k] + \begin{bmatrix} 0 \\ 0 \\ 1 \end{bmatrix} u[k] \\ y[k] &= \begin{bmatrix} (b_3 - b_0 a_3) & (b_2 - b_0 a_2) & (b_1 - b_0 a_1) \end{bmatrix} + b_0 u[k]\end{aligned}$$

where

$$\begin{aligned}\mathbf{x} &= \begin{bmatrix} x_1[k] \\ x_2[k] \\ x_3[k] \end{bmatrix}, \quad A = \begin{bmatrix} 0 & 1 & 0 \\ 0 & 0 & 1 \\ -a_3 & -a_2 & -a_1 \end{bmatrix}, \quad B = \begin{bmatrix} 0 \\ 0 \\ 1 \end{bmatrix} \\ C &= \begin{bmatrix} (b_3 - b_0 a_3) & (b_2 - b_0 a_2) & (b_1 - b_0 a_1) \end{bmatrix}, \quad D = b_0\end{aligned}$$

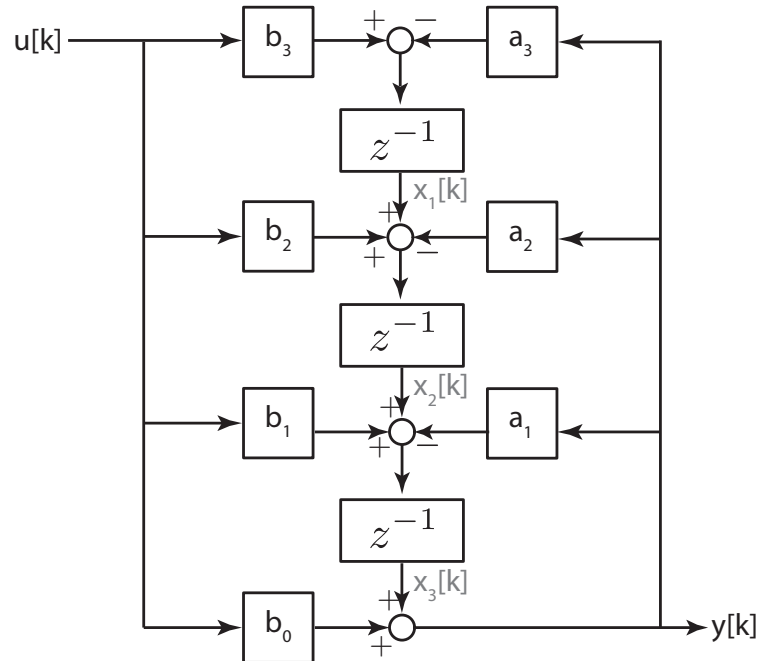
The form obtained with this approach is called reachable/controllable canonical form.

For a general n^{th} order system reachable/controllable canonical form has the following A , B , C , & D matrices

$$\begin{aligned}A &= \begin{bmatrix} 0 & 1 & 0 & \cdots & 0 \\ 0 & 0 & 1 & \cdots & 0 \\ \vdots & \vdots & \vdots & & \vdots \\ 0 & 0 & 0 & \cdots & 1 \\ -a_n & -a_{n-1} & -a_{n-2} & \cdots & -a_1 \end{bmatrix}, \quad B = \begin{bmatrix} 0 \\ 0 \\ \vdots \\ 0 \\ 1 \end{bmatrix} \\ C &= \begin{bmatrix} (b_n - b_0 a_n) & (b_{n-1} - b_0 a_{n-1}) & \cdots & (b_2 - b_0 a_2) & (b_1 - b_0 a_1) \end{bmatrix}, \quad D = b_0\end{aligned}$$

Observable Canonical Form

We also learnt a different type of canonical minimal realization which is illustrated in the Figure below



If we label the signals as given in the Figure, state evolution equations can be derived as

$$\begin{aligned} X_1(z) &= (b_3 U(z) - a_3 (U(z)b_0 + X_3(z))) z^{-1} \rightarrow x_1[k+1] = b_3 u[k] - a_3 (u[k]b_0 + x_3[k]) \\ X_2(z) &= (b_2 U(z) + X_1(z) - a_2 (U(z)b_0 + X_3(z))) z^{-1} \rightarrow x_2[k+1] = b_2 u[k] + x_1[k] - a_2 (u[k]b_0 + x_3[k]) \\ X_3(z) &= (b_1 U(z) + X_2(z) - a_1 (U(z)b_0 + X_3(z))) z^{-1} \rightarrow x_3[k+1] = b_1 u[k] + x_2[k] - a_1 (u[k]b_0 + x_3[k]) \end{aligned}$$

where as output equation can be derived as

$$y[k] = b_0 u[k] + x_3[k]$$

If we combine the state and output equations, we can obtain the state space form as

$$\begin{aligned} \mathbf{x}[k+1] &= \begin{bmatrix} 0 & 0 & -a_3 \\ 1 & 0 & -a_2 \\ 0 & 1 & -a_1 \end{bmatrix} \mathbf{x}[k] + \begin{bmatrix} b_3 - b_0 a_3 \\ b_2 - b_0 a_2 \\ b_1 - b_0 a_1 \end{bmatrix} u[k] \\ y[k] &= \begin{bmatrix} 0 & 0 & 1 \end{bmatrix} + b_0 u[k] \end{aligned}$$

where

$$\mathbf{x} = \begin{bmatrix} x_1[k] \\ x_2[k] \\ x_3[k] \end{bmatrix}, \quad A = \begin{bmatrix} 0 & 0 & -a_3 \\ 1 & 0 & -a_2 \\ 0 & 1 & -a_1 \end{bmatrix}, \quad B = \begin{bmatrix} b_3 - b_0 a_3 \\ b_2 - b_0 a_2 \\ b_1 - b_0 a_1 \end{bmatrix}, \quad C = \begin{bmatrix} 0 & 0 & 1 \end{bmatrix}, \quad D = b_0$$

The form obtained with this approach is called observable canonical form.

For a general n^{th} order system observable canonical form has the following A , B , C , & D matrices

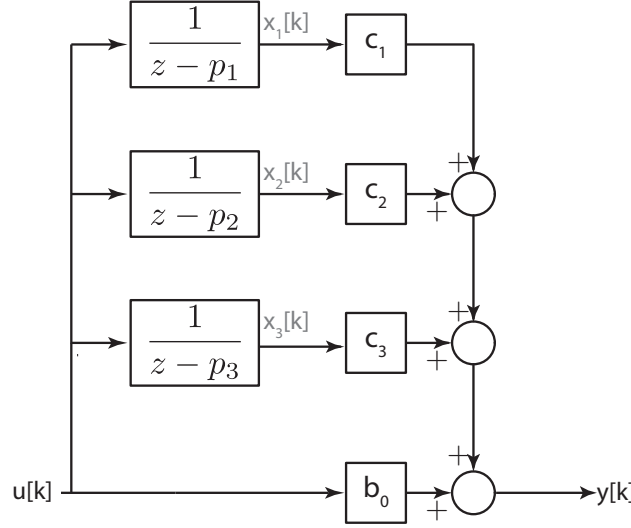
$$\begin{aligned} A &= \begin{bmatrix} 0 & 0 & \cdots & 0 & -a_n \\ 1 & 0 & \cdots & 0 & -a_{n-1} \\ \vdots & \vdots & \vdots & \vdots & \vdots \\ 0 & 0 & \cdots & 0 & -a_2 \\ 0 & 0 & \cdots & 1 & -a_1 \end{bmatrix}, \quad B = \begin{bmatrix} (b_n - b_0 a_n) \\ (b_{n-1} - b_0 a_{n-1}) \\ \vdots \\ (b_2 - b_0 a_2) \\ (b_1 - b_0 a_1) \end{bmatrix} \\ C &= \begin{bmatrix} 0 & 0 & \cdots & 0 & 1 \end{bmatrix}, \quad D = b_0 \end{aligned}$$

Diagonal Canonical Form

If the pulse transfer function of the system has distinct poles, we can expand it using partial fraction expansion

$$\begin{aligned} Y(z) &= \frac{b_0 + b_1 z^{-1} + b_2 z^{-2} + b_3 z^{-3}}{1 + a_1 z^{-1} + a_2 z^{-2} + a_3 z^{-3}} X(z) \\ &= b_0 + \frac{c_1}{z - p_1} + \frac{c_2}{z - p_2} \frac{c_3}{z - p_3} \end{aligned}$$

It is possible to realize this expanded form in block diagram form as given in the Figure below.



Now let's concentrate on the candidate "state variables" and try to write state evaluation equations

$$\begin{aligned} X_1(z) &= \frac{1}{z - p_1} U(z) \rightarrow x_1[k+1] = p_1 x_1[k] + u[k] \\ X_2(z) &= \frac{1}{z - p_2} U(z) \rightarrow x_2[k+1] = p_2 x_2[k] + u[k] \\ X_3(z) &= \frac{1}{z - p_3} U(z) \rightarrow x_3[k+1] = p_3 x_3[k] + u[k] \end{aligned}$$

where as output equation can be derived as

$$y[k] = b_0 u[k] + c_1 x_1[k] + c_2 x_2[k] + c_3 x_3[k]$$

If we combine the state and output equations, we can obtain the state space form as

$$\begin{aligned} \mathbf{x}[k+1] &= \begin{bmatrix} p_1 & 0 & 0 \\ 0 & p_2 & 0 \\ 0 & 0 & p_3 \end{bmatrix} \mathbf{x}[k] + \begin{bmatrix} 1 \\ 1 \\ 1 \end{bmatrix} u[k] \\ y[k] &= [c_1 \ c_2 \ c_3] + b_0 u[k] \end{aligned}$$

where

$$\mathbf{x} = \begin{bmatrix} x_1[k] \\ x_2[k] \\ x_3[k] \end{bmatrix}, \quad A = \begin{bmatrix} p_1 & 0 & 0 \\ 0 & p_2 & 0 \\ 0 & 0 & p_3 \end{bmatrix}, \quad B = \begin{bmatrix} 1 \\ 1 \\ 1 \end{bmatrix}, \quad C = [c_1 \ c_2 \ c_3], \quad D = b_0$$

The form obtained with this approach is called diagonal canonical form. Obviously, this form is not applicable for systems that has repeated roots.

For a general n^{th} order system with distinct roots diagonal canonical form has the following A , B , C , & D

matrices

$$A = \begin{bmatrix} p_1 & 0 & \cdots & 0 & 0 \\ 0 & p_2 & \cdots & 0 & 0 \\ \vdots & \vdots & \vdots & \vdots & \vdots \\ 0 & 0 & \cdots & p_{n-1} & 0 \\ 0 & 0 & \cdots & 0 & p_n \end{bmatrix}, \quad B = \begin{bmatrix} 1 \\ 1 \\ \vdots \\ 1 \\ 1 \end{bmatrix}$$

$$C = [c_1 \ c_2 \ \cdots \ c_{n-1} \ c_n], \quad D = b_0$$

Jordan Canonical Form

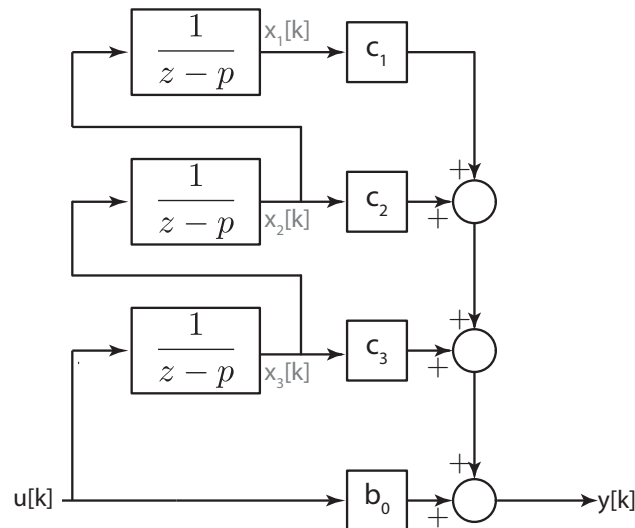
Generalization of diagonal canonical form is called Jordan canonical form which handles repeated roots.

In Jordan form the distinct roots has the same structure with Diagonal canonical form. Let's assume that the 3rd order pulse transfer function has three repeated roots. In this case, we can expand it using partial fraction expansion

$$Y(z) = \frac{b_0 + b_1 z^{-1} + b_2 z^{-2} + b_3 z^{-3}}{1 + a_1 z^{-1} + a_2 z^{-2} + a_3 z^{-3}} X(z)$$

$$= b_0 + \frac{c_1}{(z-p)^3} + \frac{c_2}{(z-p)^2} + \frac{c_3}{z-p}$$

It is possible to realize this expanded form in block diagram form as given in the Figure below.



Now let's concentrate on the candidate "state variables" and try to write state evaluation equations

$$\begin{aligned} X_1(z) &= \frac{1}{z-p} X_2(z) \rightarrow x_1[k+1] = p x_1[k] + x_2[k] \\ X_2(z) &= \frac{1}{z-p} X_3(z) \rightarrow x_2[k+1] = p x_2[k] x_3[k] \\ X_3(z) &= \frac{1}{z-p} U(z) \rightarrow x_3[k+1] = p x_3[k] + u[k] \end{aligned}$$

where as output equation can be derived as

$$y[k] = b_0 u[k] + c_1 x_1[k] + c_2 x_2[k] + c_3 x_3[k]$$

If we combine the state and output equations, we can obtain the state space form as

$$\begin{aligned} \mathbf{x}[k+1] &= \begin{bmatrix} p & 1 & 0 \\ 0 & p & 1 \\ 0 & 0 & p \end{bmatrix} \mathbf{x}[k] + \begin{bmatrix} 0 \\ 0 \\ 1 \end{bmatrix} u[k] \\ y[k] &= [c_1 \ c_2 \ c_3] + b_0 u[k] \end{aligned}$$

where

$$\mathbf{x} = \begin{bmatrix} x_1[k] \\ x_2[k] \\ x_3[k] \end{bmatrix}, \quad A = \begin{bmatrix} p & 1 & 0 \\ 0 & p & 1 \\ 0 & 0 & p \end{bmatrix}, \quad B = \begin{bmatrix} 0 \\ 0 \\ 1 \end{bmatrix}, \quad C = [c_1 \ c_2 \ c_3], \quad D = b_0$$

A , B , & C forms a Jordan block.

For a general n^{th} order system a Jordan block with m repeated roots inside a stat-space representation in Jordan canonical form looks like

$$A = \left[\begin{array}{c|ccc|cc} \ddots & & & & & & \vdots \\ \hline & \bar{p} & 1 & \cdots & 0 & 0 & 0 \\ & 0 & \bar{p} & \cdots & 0 & 0 & 0 \\ & & & \ddots & & & \\ & 0 & 0 & \cdots & \bar{p} & 1 & 0 \\ & 0 & 0 & \cdots & 0 & \bar{p} & 0 \\ \hline & & & & & \ddots & \vdots \\ \hline & \cdots & | & c_1 & c_2 & \cdots & c_{n-1} & c_n & | & \cdots \end{array} \right], \quad B = \begin{bmatrix} \vdots \\ 0 \\ 0 \\ \vdots \\ 0 \\ 1 \\ \vdots \end{bmatrix}$$

$$C = [\cdots \mid c_1 \ c_2 \ \cdots \ c_{n-1} \ c_n \mid \cdots]$$

Similarity Transformations

Consider the state-space representation of a given DT system

$$\begin{aligned} x[k+1] &= Gx[k] + Hu[k] \\ y[k] &= Cx[k] + Du[k] \end{aligned}$$

Let's define a new "state-vector" \hat{x} such that

$$\begin{aligned} Px[k] &= \hat{x}[k] \quad \text{where} \\ P &\in \mathbb{R}^{n \times n} \quad \det(P) \neq 0 \end{aligned}$$

Then we can transform the state-space equations using P as

$$\begin{aligned} P^{-1}\hat{x}[k+1] &= GP^{-1}\hat{x}[k] + Hu[k] \quad , \quad y[k] = CP^{-1}\hat{x}[k] + Du[k] \\ \hat{x}[k+1] &= PGP^{-1}\hat{x}[k] + PHu[k] \quad , \quad y[k] = CP^{-1}\hat{x}[k] + Du[k] \end{aligned}$$

The “new” state-space representation is obtained as

$$\begin{aligned} \hat{x}[k+1] &= \hat{G}\hat{x}[k] + \hat{H}u[k] \\ y[k] &= \hat{C}\hat{x}[k] + \hat{D}u[k] \\ \hat{G} &= PGP^{-1}, \quad \hat{H} = PH, \quad \hat{C} = CP^{-1}, \quad \hat{D} = D \end{aligned}$$

Since there exist infinitely many non-singular $n \times n$ matrices, for a given LTI DT system, there exist infinitely many different but equivalent state-space representations.

Example: Show that $A \in \mathbb{R}^{n \times n}$ and $P^{-1}AP$, where $P \in \mathbb{R}^{n \times n}$ and $\det(P) \neq 0$, have the same characteristic equation

Solution:

$$\begin{aligned} \det(\lambda I - P^{-1}AP) &= \det(\lambda P^{-1}IP - P^{-1}AP) \\ &= \det(P^{-1}(\lambda I - A)P) \\ &= \det(P^{-1})\det(\lambda I - A)\det(P) \\ &= \det(P^{-1})\det(P)\det(\lambda I - A) \\ \det(\lambda I - P^{-1}AP) &= \det(\lambda I - A) \end{aligned}$$

Obtaining Transfer Functions from a State-Space Representation

Let's consider the following general state-space form

$$\begin{aligned} x[k+1] &= Gx[k] + Hu[k] \\ y[k] &= Cx[k] + Du[k] \end{aligned}$$

In order to obtain transfer function form, we assume that initial conditions are zero. Under this assumption, let's take z-transform of both equations

$$\begin{aligned} zX(z) &= GX(z) + HU(z) \quad , \quad Y(z) = CX(z) + DU(z) \\ (zI - G)X(z) &= HU(z) \\ X(z) &= (zI - G)^{-1}HU(z) \\ Y(z) &= C(zI - G)^{-1}HU(z) + DU(z) \\ Y(z) &= \left[C(zI - G)^{-1}H + D \right] U(z) \\ T(z) &= \left[C(zI - G)^{-1}H + D \right] \end{aligned}$$

If the system is a SISO system, then $T(z)$ is a transfer function, whereas for MIMO case $T(z)$ becomes a *transfer function matrix*. Note that $(zI - G)^{-1}$ is invertible for all $z \in \mathbb{C}$ except the eigenvalues of G .

Example: Let p be a pole of $T(z)$, show that p is also an eigenvalue of G .

Solution: Let

$$T(z) = \frac{n(z)}{d(z)}$$

If p is a pole of $T(z)$, then $d(z)|_p = 0$. Now let's analyze the dependence of $T(z)$ to the state-space form.

$$\begin{aligned} T(z) &= \left[C(zI - G)^{-1} H + D \right] \\ (zI - G)^{-1} &= \frac{\text{Adj}(zI - G)}{\det(zI - G)} \\ T(z) &= \frac{C \text{Adj}(zI - G) H + D \det(zI - G)}{\det(zI - G)} \end{aligned}$$

If p is a pole of $T(z)$, then

$$\det(zI - G)|_{z=p} = 0$$

Obviously p is an eigenvalue of G .

Invariance of Transfer Functions Under Similarity Transformation

Consider the two different state-space representations

$$\begin{aligned} x[k+1] &= Gx[k] + Hu[k] & \hat{x}[k+1] &= \hat{G}\hat{x}[k] + \hat{H}u[k] \\ y[k] &= Cx[k] + Du[k] & y[k] &= \hat{C}\hat{x}[k] + \hat{D}u[k] \end{aligned}$$

where they are related with the following similarity transformation

$$Px[k] = \hat{x}[k], \quad \hat{G} = PGP^{-1}, \quad \hat{H} = PH, \quad \hat{C} = CP^{-1}, \quad \hat{D} = D$$

Let's compute the transfer function for the second representation

$$\begin{aligned} \hat{T}(z) &= \left[\hat{C} \left(zI - \hat{G} \right)^{-1} \hat{H} + \hat{D} \right] \\ &= \left[CP^{-1} \left(zI - PGP^{-1} \right)^{-1} PH + D \right] \\ &= \left[CP^{-1} \left(P(zI - G)P^{-1} \right)^{-1} PH + D \right] \\ &= \left[CP^{-1}P(zI - G)^{-1}P^{-1}PH + D \right] \\ &= \left[C(zI - G)^{-1}H + D \right] \\ \hat{T}(z) &= T(z) \end{aligned}$$

Solution of Discrete-Time State-Space Equations

Let's first assume that $u[k] = 0$, and find un-driven (homogeneous) response.

$$\begin{aligned} x[k+1] &= Gx[k] \\ y[k] &= Cx[k] \end{aligned}$$

Unlike CT systems we can compute the response iteratively

$$\begin{aligned} x[1] &= Gx[0] \\ x[2] &= Gx[1] = G^2x[0] \\ x[3] &= Gx[2] = G^3x[0] \\ &\vdots \\ x[k] &= Gx[k-1] = G^kx[0] \quad , \quad y[k] = CG^kx[0] \end{aligned}$$

It is easy to see that for $k, p \in \mathbb{Z}$ where $k > p$

$$x[k] = G^{k-p}x[p]$$

Let $\Psi(k) = G^k$, then this matrix of functions solves the homogeneous difference equation

$$\begin{aligned} x[k+1] &= Gx[k] \\ x[k] &= \Psi[k]x[0] \\ x[k] &= \Psi[k-p]x[p] \\ x[k+m] &= \Psi[k+m-m]x[m] = \Psi[k] \end{aligned}$$

$\Psi[k]$ is called the state-transition matrix. Now let's consider input-only state response (i.e. $x[0] = 0$).

$$x[k+1] = Gx[k] + Hu[k]$$

$$\begin{aligned} x[1] &= Hu[0] \\ x[2] &= Gx[1] + Hu[1] = GHu[0] + Hu[1] \\ x[3] &= Gx[2] + Hu[2] = G^2Hu[0] + GHu[1] + Hu[2] \\ x[4] &= Gx[3] + Hu[3] = G^3Hu[0] + G^2Hu[1] + GHu[2] + Hu[3] \\ &\vdots \\ x[k] &= Gx[k-1] + Hu[k-1] \\ &= G^{k-1}Hu[0] + G^{k-2}Hu[1] + \cdots + GHu[k-2] + Hu[k-1] \\ &= [\quad G^{k-1}H \mid G^{k-2}H \mid \cdots \mid GH \mid H \quad] \begin{bmatrix} u[0] \\ u[1] \\ \vdots \\ u[k-2] \\ u[k-1] \end{bmatrix} \\ &= \sum_{j=0}^{k-1} G^{k-j-1}Hu[j] \\ &= \sum_{j=0}^{k-1} G^jHu[k-j-1] \end{aligned}$$

Given that $\Psi[k] = G^k$

$$\begin{aligned} x[k] &= \sum_{j=0}^{k-1} \Psi[k-j-1]Hu[j] \\ &= \sum_{j=0}^{k-1} \Psi[j]Hu[k-j-1] \end{aligned}$$

If we combine homogeneous and driven responses we can simply obtain

$$\begin{aligned} x[k] &= \Psi[k]x[0] + \sum_{j=0}^{k-1} \Psi[k-j-1]Hu[j] \\ &= \Psi[k]x[0] + \sum_{j=0}^{k-1} \Psi[j]Hu[k-j-1] \end{aligned}$$

whereas output at time k has the form

$$\begin{aligned} y[k] &= C\Psi[k]x[0] + C \left(\sum_{j=0}^{k-1} \Psi[k-j-1]Hu[j] \right) Du[k] \\ &= C\Psi[k]x[0] + C \left(\sum_{j=0}^{k-1} \Psi[j]Hu[k-j-1] \right) Du[k] \end{aligned}$$

Z-domain Solution of State-Space Equations

We already computed the transfer function under zero initial conditions.

$$Y(z) = \left[C(zI - G)^{-1} H + D \right] U(z)$$

Now let's compute the response to initial condition in Z-domain.

$$\begin{aligned}\mathcal{Z}[x[k+1]] &= \mathcal{Z}[Gx[k]] \\ zX(z) - zx[0] &= GX(z) \\ (zI - G)X(z) &= zX(z) \\ X(z) &= z(zI - G)^{-1}x[0]\end{aligned}$$

Similarly $Y(z)$ takes the form

$$Y(z) = zC(zI - G)^{-1}x[0]$$

We can also observe that

$$\begin{aligned}\mathcal{Z}[\Psi[k]] &= \mathcal{Z}[G^k] = z(zI - G)^{-1} \\ \mathcal{Z}^{-1}[z(zI - G)^{-1}] &= \Psi[k] = G^k\end{aligned}$$

If we expand $z(zI - G)^{-1}$ by long “division” we can also observe the relation in z-domain and time domain expressions from different perspective

$$\begin{array}{c|cc} z & | & zI - G \\ \hline zI - G & | & I + z^1G + z^2G^2 + z^3G^3 + \dots \\ \hline & G \\ & G - z^{-1}G^2 \\ \hline & z^{-1}G^2 \\ & z^{-1}G^2 - z^{-2}G^3 \\ \hline & z^{-2}G^3 \\ & \vdots \end{array}$$

$$\begin{aligned}z(zI - G)^{-1} &= I + z^{-1}G + z^{-2}G^2 + z^{-3}G^3 + \dots \\ \mathcal{Z}\left[z(zI - G)^{-1}\right] &= \{I, G, G^2, G^3, \dots\}\end{aligned}$$

Example: Consider the following state-space representation

$$\begin{aligned}x[k+1] &= \begin{bmatrix} 1 & 0 & 0 \\ 0 & 1/2 & 0 \\ 0 & 0 & -1 \end{bmatrix} x[k] + \begin{bmatrix} 1 \\ 1 \\ 1 \end{bmatrix} u[k] \\y[k] &= [1 \ 2 \ 3] x[k]\end{aligned}$$

- Compute the closed form expression $\Psi[k]$ using the time expression

Solution: The state-space representation is in Diagonal canonical form

$$\Psi[k] = G^k = \begin{bmatrix} 1 & 0 & 0 \\ 0 & 1/2 & 0 \\ 0 & 0 & -1 \end{bmatrix}^k = \begin{bmatrix} 1^k & 0 & 0 \\ 0 & (1/2)^k & 0 \\ 0 & 0 & (-1)^k \end{bmatrix} = \begin{bmatrix} 1 & 0 & 0 \\ 0 & (1/2)^k & 0 \\ 0 & 0 & (-1)^k \end{bmatrix}$$

- Compute the closed form expression $\Psi[k]$ using the z-domain solution method

Solution:

$$\begin{aligned}\Psi[k] &= \mathcal{Z}^{-1} \left[z(zI - G)^{-1} \right] \\&= \mathcal{Z}^{-1} \left[z \left(\begin{bmatrix} z-1 & 0 & 0 \\ 0 & (z-1/2) & 0 \\ 0 & 0 & z+1 \end{bmatrix} \right)^{-1} \right] \\&= \mathcal{Z}^{-1} \left[\begin{bmatrix} \frac{z}{z-1} & 0 & 0 \\ 0 & \frac{z}{z-1/2} & 0 \\ 0 & 0 & \frac{z}{z+1} \end{bmatrix} \right] \\&= \begin{bmatrix} 1 & 0 & 0 \\ 0 & (1/2)^k & 0 \\ 0 & 0 & (-1)^k \end{bmatrix} \quad \text{for } k \geq 0\end{aligned}$$

- Compute the impulse response of the system from the time domain solution

Solution:

$$\begin{aligned}x[k] &= G^{k-1} H u[0] \quad \text{for } k > 0 \\y[k] &= C G^{k-1} H \quad \text{for } k > 0 \\&= [1 \ 2 \ 3] \begin{bmatrix} 1 & 0 & 0 \\ 0 & (1/2)^{k-1} & 0 \\ 0 & 0 & (-1)^{k-1} \end{bmatrix} \begin{bmatrix} 1 \\ 1 \\ 1 \end{bmatrix} \\&= [1 \ 2 \ 3] \begin{bmatrix} 1 \\ (1/2)^{k-1} \\ (-1)^{k-1} \end{bmatrix} \\y[k] &= 1 + 2(1/2)^{k-1} + 3(-1)^{k-1} \quad \text{for } k > 0\end{aligned}$$

- Compute the transfer function $\frac{Y(z)}{U(z)}$

Solution:

$$\begin{aligned}
 T(z) &= C(zI - G)^{-1} H \\
 &= [1 \ 2 \ 3] \begin{bmatrix} z-1 & 0 & 0 \\ 0 & z-1/2 & 0 \\ 0 & 0 & z+1 \end{bmatrix}^{-1} \begin{bmatrix} 1 \\ 1 \\ 1 \end{bmatrix} \\
 &= [1 \ 2 \ 3] \begin{bmatrix} \frac{1}{z-1} & 0 & 0 \\ 0 & \frac{1}{z-1/2} & 0 \\ 0 & 0 & \frac{1}{z+1} \end{bmatrix} \begin{bmatrix} 1 \\ 1 \\ 1 \end{bmatrix} \\
 &= [1 \ 2 \ 3] \begin{bmatrix} \frac{1}{z-1} \\ \frac{1}{z-1/2} \\ \frac{1}{z+1} \end{bmatrix} \\
 T(z) &= \frac{1}{z-1} + \frac{2}{z-1/2} + \frac{3}{z+1}
 \end{aligned}$$

- Compute the inverse Z-transform of the transfer function

Solution:

$$\begin{aligned}
 t[k] &= \mathcal{Z}^{-1} \left[\frac{1}{z-1} + \frac{2}{z-1/2} + \frac{3}{z+1} \right] \\
 &= (1 + 2(1/2)^{k-1} + 3(-1)^{k-1}) h[k-1]
 \end{aligned}$$

where $h[k]$ is the unit step function